# n-Lüders channels: A novel class of rebit channels and their properties

Michel Berthier, Edoardo Provenzi

# $n$-Lüders channels: A novel class of rebit channels and their properties

Michel Berthier*[1] and Edoardo Provenzi†[2]

[1]Laboratoire MIA, Batiment Pascal, Pôle Sciences et Technologie, Université de La Rochelle, 23, Avenue A. Einstein, BP 33060, 17031 La Rochelle cedex, France
[2]Université de Bordeaux, CNRS, Bordeaux INP, IMB, UMR 5251, F-33400, 351 Cours de la Libération, Talence, France

**Abstract**

In a very recent paper, the complete classification of rebit channels has been achieved. Here, we exploit that result to show how the classification can be used to perform an exhaustive analyze a novel class of rebit channels induced by effects called $n$-Lüders channels. In the final part of the paper we propose a concrete application of these channels within the mathematical framework of a quantum theory of color perception that originated the interest about a rebit channels classification.

As discussed in a very recent paper, while the complete classification of *qubit channels* has been known since 2002, see [23], a similar accomplishment for *rebit channels* has not been obtained until 2023 in [1]. This temporal gap is probably due to the lack of concrete examples of *physical* rebit systems, which, nevertheless, continue to inspire very insightful theoretical studies, see e.g. [2, 14, 18, 19, 21, 26, 27] just to have a few examples.

Since 2019, a concrete example of rebit system became available not from the study of physics, but from psycho-physics, in particular, the modeling of color perception. While this fact may seem surprising, a very brief historical recap of color research will show how this discipline and mathematical physics are close to each other. In fact, during the golden era of research about color perception, the eighteenth and nineteenth centuries, mathematical and theoretical physicists of the caliber of Newton, Maxwell and von Helmholtz, and first rank mathematicians such as Riemann and Grassmann, established the first law of color perception and the first hints about the properties verified by the space that should contain color percepts. Their results were brilliantly resumed and axiomatized by Schrödinger in 1920, see [24], and further refined by Resnikoff in 1974, see [22].

This shows that, at least in its beginning, color research was considered as a genuine branch of mathematical physics, the only difference with 'ordinary' physics being that the data to be mathematically modeled with precise laws did not came from measurements performed via hand-made instruments, but using the humans visual system, whose *statistical robustness* guarantees the possibility of a mathematical modeling and the determination of precise laws. Starting from these premises, color perception data can be gathered in abstract structures with known mathematical properties which, in turn, allow scientists a deeper exploration of intrinsic properties and the possibility to make novel predictions about phenomena not yet measured. To distinguish it from ordinary mathematical physics, we propose the definition '*mathematical psycho-physics*' for the rigorous study of perceptual phenomena.

As it can be seen in the papers [6, 4, 9, 5, 7, 8, 10], listed in chronological order, once the original work of the founding fathers of color research is interpreted from a quantum information

*michel.berthier@univ-lr.fr
†edoardo.provenzi@math.u-bordeaux.fr

viewpoint, then a rebit system comes out naturally to represent the space of chromatic states. The motivations underlying a quantum approach to color perception have been thoroughly discussed in [5].

The complete classification of rebit channels achieved in [1] was actually inspired by some theoretical questions of this novel theory of color perception. In this paper, we propose another mathematically rigorous study inspired by this color perception theory, but, this time, related to a specific class of quantum channels that will be called *n-Lüders channels*. The reason for this particular name comes from a transformation induced by a fundamental object of quantum information theory: the effect. It is well-known, see e.g. [11] for more details, that effect label the so-called Lüders operations, which are completely positive transformations between Hilbert state spaces analytically expressed as the double-sided product of a density matrix with the square root of the effect operator. Lüders operations are not quantum channels because they are not trace preserving, so they do not map states into states, rather, they transform states into so-called *generalized states*.

After recalling the mathematical preliminaries needed for the remaining part of the paper in section 1, we use the Kraus decomposition theorem to show what prevents Lüders operations to be channels and we propose the easiest possible modification in order to build channels from Lüders operations. We also show that, if we consider $n$ effects instead of a single one, with a suitable linear combination we can still built channels, this explains the presence of the number $n$ in the definition of Lüders effects.

In section 3, we will exhibit the general action of $n$-Lüders channels of Bloch vectors which, in section 4, will allow us determining, together with the classification of rebit channels, what kind of rebit channels can be represented by $n$-Lüders channels. In particular, we will show that $n$-Lüders channels do not exhaust all rebit channels and that, quite peculiarly, when $n = 1$ only a very particular class of them can be represented, instead, from $n = 2$ on, all types (but not all) of rebit channels can be represented by $n$-Lüders channels.

These results can be obtained not only thanks to the classification of rebit channels, but also to the theorems proven in [10] about rebit systems. So, the extension of $n$-Lüders channels to qubit systems, although very interesting, is not immediate and requires a dedicated analysis. This is why we preferred to conclude the paper, in section 5, with the discussion of some applications of $n$-Lüders channels to the theory of color perception that originated their study.

# 1 Mathematical preliminaries

Let $A$ be an open quantum system with Hilbert state space $\mathcal{H}_A$ able to interact with its environment represented by a system $B$ with Hilbert state space $\mathcal{H}_B$. Both $\mathcal{H}_A$ and $\mathcal{H}_B$ are supposed to be finite-dimensional.

If $L(\mathcal{H}_A)$ is the vector space of linear operators on $\mathcal{H}_A$, then a linear map $\psi : L(\mathcal{H}_A) \to L(\mathcal{H}_A)$ is said to be an *operation* of the system $A$ if it is completely positive, i.e. if both $\psi$ and its $B$-extension, i.e. the map $\psi \otimes id_B : L(\mathcal{H}_A \otimes \mathcal{H}_B) \to L(\mathcal{H}_A \otimes \mathcal{H}_B)$, preserve the positivity of operators upon which they act[1]. If an operation $\psi$ is also trace-preserving, then it is called a *channel* and indicated with $C$.

The requests defining a channel $C$ are the minimal ones to guarantee that $C$ maps states into states and that $C$ does not introduce non-meaningful negative probabilities when experiments on the composite quantum system $A + B$ are performed.

Since in this paper we are interested in rebit systems, from now on we will identify the Hilbert state space $\mathcal{H}_A$ with $\mathbb{R}^2$. As it is well-known, the density matrices representing rebit states $\mathbf{s}$ are unit trace positive semi-definite matrices and they can be written as follows

$$\rho_{\mathbf{s}}(s_1, s_2) = \frac{1}{2} \begin{pmatrix} 1 + s_1 & s_2 \\ s_2 & 1 - s_1 \end{pmatrix}, \tag{1}$$

[1]Given a generic Hilbert space $\mathcal{H}$ with inner product $\langle\ ,\ \rangle_{\mathcal{H}}$ and $T \in L(\mathcal{H})$, $T$ is positive if, for all $x \in \mathcal{H}$, $\langle x, Tx\rangle_{\mathcal{H}} \geq 0$ .

with the constraint $s_1^2 + s_2^2 \leq 1$. Hence, the state space of a rebit system, denoted with the symbol $\mathcal{S}(\mathbb{R}^2) \subset L(\mathbb{R}^2)$, can be parameterized by the points of the unit disk $\mathcal{D}$ in $\mathbb{R}^2$, usually called *Bloch disk*. The reason for this name relies in the well-known Bloch decomposition of $\rho_{\mathbf{s}}$, i.e.

$$\rho_{\mathbf{s}} = \frac{1}{2}(\sigma_0 + \mathbf{v}_{\mathbf{s}} \cdot \vec{\sigma}) \equiv \rho_0 + s_1\sigma_1 + s_2\sigma_2, \tag{2}$$

where $\sigma_0 = I_2$, $\sigma_1$ and $\sigma_2$, the real Pauli matrices

$$\sigma_1 = \begin{pmatrix} 1 & 0 \\ 0 & -1 \end{pmatrix},\ \sigma_2 = \begin{pmatrix} 0 & 1 \\ 1 & 0 \end{pmatrix}, \tag{3}$$

form the *Bloch basis* of $\mathcal{H}(2, \mathbb{R})$, the vector space of $2 \times 2$ real symmetric matrices. $\rho_0 = I_2/2$ represents the *maximally mixed rebit state* and $\mathbf{v}_{\mathbf{s}} = (s_1, s_2)^t \in \mathcal{D}$ is the *Bloch vector* associated to $\rho_{\mathbf{s}}$. The state $\mathbf{s}$ is *pure* if and only if $\|\mathbf{v}_{\mathbf{s}}\| = 1$, so that pure rebit states are parameterized by the border of the Bloch disk, i.e. $S^1$, the unit circle.

A fine descriptor of mixedness of a state $\mathbf{s}$ is its *von Neumann entropy*, defined by:

$$S(\rho_{\mathbf{s}}) := -\operatorname{Tr}(\rho_{\mathbf{s}} \log_2 \rho_{\mathbf{s}}) = -\sum_k \lambda_k \log_2 \lambda_k, \tag{4}$$

where the real numbers $\lambda_k$ are the strictly positive eigenvalues of $\rho_{\mathbf{s}}$, repeated as many times in the sum as their algebraic multiplicity. In the rebit case they are $\lambda_1 = (1 - r_{\mathbf{s}})/2$ and $\lambda_2 = (1 + r_{\mathbf{s}})/2$, where $r_{\mathbf{s}} = \|\mathbf{v}_{\mathbf{s}}\|$.

All rebit channels $C$ preserve the space state, i.e. $C(\mathcal{S}(\mathbb{R}^2)) \subseteq \mathcal{S}(\mathbb{R}^2)$, but an arbitrary rebit operation $\psi$ fails to do that, i.e. $\mathcal{S}(\mathbb{R}^2) \subseteq \psi(\mathcal{S}(\mathbb{R}^2))$, because $\psi$ reduces the trace of density matrices to a value belonging to $[0, 1]$, interpreted as probabilities. The range of rebit operations is called the space of *generalized rebit states*.

A noticeable class of operations can be built thanks to the concept of *effect*, which is the image of a positive operator-valued measure and it embodies the probabilistic nature of quantum measurement, see e.g. the classic references [11, 12] for more details about this fundamental concept.

In the rebit case, a generic effect $\mathbf{e}$ can be represented by the following matrix

$$\eta_{\mathbf{e}} = \begin{pmatrix} e_0 + e_1 & e_2 \\ e_2 & e_0 - e_1 \end{pmatrix}, \tag{5}$$

with the coefficients $e_0, e_1, e_2 \in \mathbb{R}$ satisfying the double constraint $\mathbf{0} \leq \eta_{\mathbf{e}} \leq I_2$. By making the constraints explicit one finds the *effect space* of a rebit system:

$$\mathcal{E} = \left\{ \mathbf{e} = (e_0, e_1, e_2) \in \mathbb{R}^3,\ e_0 \in [0, 1],\ e_1^2 + e_2^2 \leq \min_{e_0 \in [0,1]} \left\{ (1 - e_0)^2, e_0^2 \right\} \right\}. \tag{6}$$

As it can be seen in Figure 1, $\mathcal{E}$ is a closed convex double cone with a circular basis of radius $1/2$ located height $e_0 = 1/2$ and vertices in $(0, 0, 0)$ and $(1, 0, 0)$, associated to the *null* and *unit effect*, respectively.

Following the nomenclature established in [10], we call $e_0 \in [0, 1]$ *effect magnitude* and, whenever $e_0 \neq 0$, we call

$$\mathbf{v}_{\mathbf{e}} = \left( \frac{e_1}{e_0}, \frac{e_2}{e_0} \right)^t \in \mathcal{D} \tag{7}$$

*effect vector*.

The *Lüders operation* $\psi_{\mathbf{e}}$ induced by an effect $\mathbf{e}$ transforms a density matrix $\rho_{\mathbf{s}}$ into the so-called *post-measurement generalized state* defined by

$$\psi_{\mathbf{e}}(\mathbf{s}) = \eta_{\mathbf{e}}^{1/2} \rho_{\mathbf{s}} \eta_{\mathbf{e}}^{1/2}, \tag{8}$$

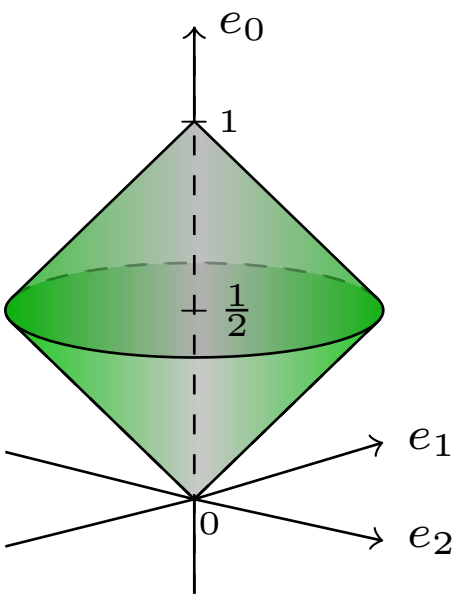


Figure 1: The effect space $\mathcal{E}$ of a rebit system.

see e.g. [11] page 37, where $\eta_{\mathbf{e}}^{1/2}$ is the square root of $\eta_{\mathbf{e}}$, i.e. the only symmetric and positive semi-definite matrix such that $\eta_{\mathbf{e}}^{1/2}\eta_{\mathbf{e}}^{1/2} = \eta_{\mathbf{e}}$. Thanks to the cyclic property of the trace we have:

$$\mathrm{Tr}(\psi_{\mathbf{e}}(\mathbf{s})) = \mathrm{Tr}(\rho_{\mathbf{s}}\,\eta_{\mathbf{e}}) = \langle \mathbf{e} \rangle_{\mathbf{s}} = e_0(1 + \mathbf{v_e} \cdot \mathbf{v_s}), \tag{9}$$

where $\langle \mathbf{e} \rangle_{\mathbf{s}}$ is the expectation value of the effect $\mathbf{e}$ on the state $\mathbf{s}$ and the dot symbol denotes the Euclidean inner product between vectors. It follows that

$$\varphi_{\mathbf{e}}(\mathbf{s}) := \frac{\psi_{\mathbf{e}}(\mathbf{s})}{\mathrm{Tr}(\psi_{\mathbf{e}}(\mathbf{s}))} \tag{10}$$

is a density matrix corresponding to a rebit state.

In [10], the post-measurement Bloch vector relative to $\varphi_{\mathbf{e}}(\mathbf{s})$ has been proven to be the Einstein-Poincaré relativistic sum of $\mathbf{v_e}$ and $\mathbf{v_s}$, i.e.

$$\mathbf{v}_{\varphi_{\mathbf{e}}(\mathbf{s})} = \mathbf{v_e} \oplus \mathbf{v_s}, \tag{11}$$

where the relativistic sum $\mathbf{v_e} \oplus \mathbf{v_s}$ is defined as follows (see e.g. [25]): if $\|\mathbf{v_e}\| < 1$, then

$$\mathbf{v_e} \oplus \mathbf{v_s} := \frac{1}{1 + \mathbf{v_e} \cdot \mathbf{v_s}} \left\{ \mathbf{v_e} + \frac{1}{\gamma_{\mathbf{v_e}}}\mathbf{v_s} + \frac{\gamma_{\mathbf{v_e}}}{1 + \gamma_{\mathbf{v_e}}}(\mathbf{v_e} \cdot \mathbf{v_s})\mathbf{v_e} \right\}, \tag{12}$$

where $\gamma_{\mathbf{v_e}}$ is the Lorentz factor defined by

$$\gamma_{\mathbf{v_e}} := \frac{1}{\sqrt{1 - \|\mathbf{v_e}\|^2}}, \tag{13}$$

and, if $\|\mathbf{v_e}\| = 1$,

$$\mathbf{v_e} \oplus \mathbf{v_s} := \mathbf{v_e}. \tag{14}$$

We consider important to remark that eq. (11) is not merely the accidental result of a technical computation, but it has more profound roots: in fact, it relies on the existence of a relevant Jordan algebra isomorphism between the Jordan algebra of real symmetric $2 \times 2$ matrices $\mathcal{H}(2, \mathbb{R})$ and

the spin factor $\mathbb{R} \oplus \mathbb{R}^2$, both endowed with their respective Jordan product, see e.g. [3] for further information.

From eqs. (10) and (11) we can define the vector associated to $\psi_{\mathbf{e}}(\mathbf{s})$ as

$$\mathbf{v}_{\psi_{\mathbf{e}}(\mathbf{s})} := \mathrm{Tr}(\psi_{\mathbf{e}}(\mathbf{s}))\, \mathbf{v}_{\mathbf{e}} \oplus \mathbf{v}_{\mathbf{s}} = e_0(1 + \mathbf{v}_{\mathbf{e}} \cdot \mathbf{v}_{\mathbf{s}})\mathbf{v}_{\mathbf{e}} \oplus \mathbf{v}_{\mathbf{s}}. \tag{15}$$

We end the recap of the mathematical results that will be used in the following sections by quoting the classification theorem of rebit channels obtained in [1].

**Theorem 1.1** *Every rebit channel $C : L(\mathbb{R}^2) \to L(\mathbb{R}^2)$ can be decomposed as follows:*

$$C = \sigma_{\Omega_{\mathcal{R}_1}} \circ C_D \circ \sigma_{\Omega_{\mathcal{R}_2}}, \tag{16}$$

*where:*

- *$\sigma_{\Omega_{\mathcal{R}_j}}$ are called orthogonal channels and they act on $L(\mathbb{R}^2)$ by conjugation with the rotation matrices $\mathcal{R}_j \in \mathrm{SO}(2)$, $j = 1, 2$, i.e. $\sigma_{\Omega_{\mathcal{R}_j}}(T) = \mathcal{R}_j T {\mathcal{R}_j}^t$, for all $T \in L(\mathbb{R}^2)$;*
- *$C_D$ can be represented in the Bloch basis $(\sigma_0, \sigma_1, \sigma_2)$ by the affine matrix*

$$\mathbb{A} = \begin{pmatrix} 1 & 0 & 0 \\ w_1 & \lambda_1 & 0 \\ w_2 & 0 & \lambda_2 \end{pmatrix} = \begin{pmatrix} 1 & \mathbf{0} \\ \mathbf{w} & D \end{pmatrix},$$

*with the coefficients $\lambda_j, w_j$, $j = 1, 2$, satisfying the following constraints:*

$$\begin{cases} 1 + \lambda_1 + \lambda_2 \geq 0 \\ 1 + \lambda_1 - \lambda_2 \geq 0 \\ 1 - \lambda_1 + \lambda_2 \geq 0 \\ \frac{w_1^2}{(1+\lambda_1+\lambda_2)(1+\lambda_1-\lambda_2)} + \frac{w_2^2}{(1+\lambda_1+\lambda_2)(1-\lambda_1+\lambda_2)} \leq 1 \end{cases} . \tag{17}$$

$C_D$ shrinks the whole Bloch disk into an ellipsoidal region contained in $\mathcal{D}$, which can also degenerate into a line segment or even a point.

$C$ is a *unital channel* if it preserves the identity map or, when restricted to $\mathcal{S}(\mathbb{R}^2)$, if $C(\rho_0) = \rho_0$. Of course $C$ can be unital if and only if $\mathbf{w} = \mathbf{0}$, otherwise $C(\mathcal{D})$ is an ellipsoid with center shifted by $\mathbf{w}$ with respect to the origin.

Up to rotations, the action of unital channels is described by the diagonal part $C_D$, which is parameterized by the two coefficients $\lambda_1, \lambda_2$ satisfying the first three constraint appearing in the system of inequalities (17), which guarantee the complete positiveness of the map $C_D$ in the unital case. The part of the real plane delimited by these constraints is called *admissibility region*, denoted with $\mathcal{P}$ and exhibited in Figure 2.

# 2 Definition of $n$-Lüders channels

The novel class of channels that we are going to define and study in this section is built from Lüders operations. It must be first underlined that, even if $\varphi_{\mathbf{e}}(\mathbf{s})$ is a state for all effect $\mathbf{e}$, the transformation $\mathbf{s} \mapsto \varphi_{\mathbf{e}}(\mathbf{s})$ is *not* a rebit channel unless $\mathbf{e} = (1, 0, 0)$ or, equivalently, $\eta_{\mathbf{e}} = I_2$. This can be easily proven using the *Kraus decomposition theorem*, see e.g. [15] page 188, which implies that, if $\mathcal{H}$ is a generic real Hilbert space, a $\mathbb{R}$-linear map $C : L(\mathcal{H}) \to L(\mathcal{H})$ is a channel if and only if there exists a finite or countable infinite sequence of bounded $\mathbb{R}$-linear operators $(A_k)_{k \in \mathbb{N}}$ on $\mathcal{H}$ satisfying:

$$\sum_{k \in \mathbb{N}} A_k^t A_k = id_{\mathcal{H}} \tag{18}$$

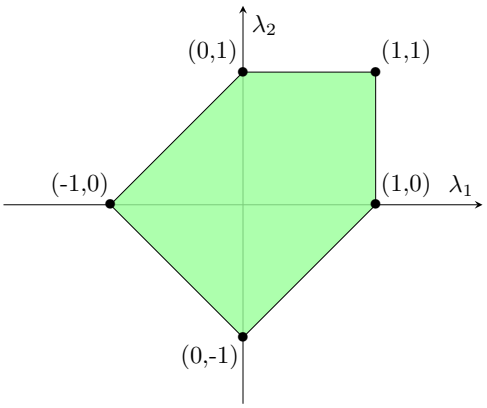


Figure 2: Admissibility region $\mathcal{P}$ for the parameters $\lambda_1$ and $\lambda_2$ that label all diagonal rebit channels $C_D$.

such that $C$ can be decomposed in the following *Kraus form*:

$$C(T) = \sum_{k\in\mathbb{N}} A_k T A_k^t, \qquad \forall T \in L(\mathcal{H}). \tag{19}$$

Due to the symmetry of $\eta_{\mathbf{e}}$, the only possible Kraus form of $\varphi_{\mathbf{e}}(\mathbf{s})$ is:

$$\varphi_{\mathbf{e}}(\mathbf{s}) = \frac{\eta_{\mathbf{e}}^{1/2}}{\sqrt{\langle\mathbf{e}\rangle_{\mathbf{s}}}}\rho_{\mathbf{s}}\frac{\eta_{\mathbf{e}}^{1/2}}{\sqrt{\langle\mathbf{e}\rangle_{\mathbf{s}}}}, \tag{20}$$

and so the constraint (18) imposes

$$\frac{\eta_{\mathbf{e}}}{\langle\mathbf{e}\rangle_{\mathbf{s}}} = I_2, \tag{21}$$

which is satisfied *for all states* $\mathbf{s}$ if and only if $e_0 = 1$ and $e_1 = e_2 = 0$.

Nevertheless, as we are going to show, Lüders operations can be used to build channels. Given $n$ effects, $\mathbf{e}_j = ((e_j)_0, (e_j)_1, (e_j)_2) \in \mathcal{E}$, $j = 1, \ldots, n$, where $n \in \mathbb{N}$, $n \geq 1$, it is straightforward to verify that also

$$\mathbb{1} - \mathbf{e}_j := (1 - (e_j)_0, -(e_j)_1, -(e_j)_2), \qquad j = 1, \ldots, n, \tag{22}$$

are effects. For every fixed $j$, the matrix associated to $\mathbb{1} - \mathbf{e}_j$ is

$$\eta_{\mathbb{1}-\mathbf{e}_j} = \begin{pmatrix} 1 - (e_j)_0 - (e_j)_1 & -(e_j)_2 \\ -(e_j)_2 & 1 - (e_j)_0 + (e_j)_1 \end{pmatrix} = I_2 - \eta_{\mathbf{e}_j}, \tag{23}$$

and the effect vector associated to $\mathbb{1} - \mathbf{e}_j$ is

$$\mathbf{v}_{\mathbb{1}-\mathbf{e}_j} = \left(-\frac{(e_j)_1}{1 - (e_j)_0}, -\frac{(e_j)_2}{1 - (e_j)_0}\right) = -\frac{(e_j)_0}{1 - (e_j)_0}\mathbf{v}_{\mathbf{e}_j} \in \mathcal{D}, \tag{24}$$

so $\mathbf{v}_{\mathbf{e}}$ and $\mathbf{v}_{\mathbb{1}-\mathbf{e}}$ are collinear, but they point to opposite directions. Moreover, they are simultaneously well-defined if and only if

$$(e_j)_0 \in (0, 1), \tag{25}$$

from now on, the condition expressed in eq. (25) will be implicitly assumed. This means that the unit and null effects, located at the top and bottom vertices of the double cone $\mathcal{E}$, respectively, will not intervene in the analysis of the channels that we are going to define. Finally, even if we concentrate on their action on $\mathcal{S}(\mathbb{R}^2)$, their definition can be extended to $L(\mathbb{R}^2)$ by linearity.

**Def. 2.1 ($n$-Lüders channel)** *Let $n \geq 1$ and consider the effects $\mathbf{e}_j \in \mathcal{E}$, $j = 1, \ldots, n$. Then, the $n$-Lüders channel $\mathcal{L}_{\mathbf{e}_1,\ldots,\mathbf{e}_n}$ induced by these effects acts on states as follows:*

$$\mathcal{L}_{\mathbf{e}_1,\ldots,\mathbf{e}_n}(\mathbf{s}) := \frac{1}{n}\sum_{j=1}^{n}\left[\psi_{\mathbf{e}_j}(\mathbf{s}) + \psi_{\mathbb{1}-\mathbf{e}_j}(\mathbf{s})\right], \tag{26}$$

*where, for every fixed $j$, $\psi_{\mathbf{e}_j}$ and $\psi_{\mathbb{1}-\mathbf{e}_j}$ are the Lüders operations corresponding to the effect $\mathbf{e}_j$ and $\mathbb{1} - \mathbf{e}_j$, respectively.*

It follows immediately that the action of $\mathcal{L}_{\mathbf{e}_1,\ldots,\mathbf{e}_n}$ on density matrices is given by

$$\mathcal{L}_{\mathbf{e}_1,\ldots,\mathbf{e}_n}(\rho_{\mathbf{s}}) := \frac{1}{n}\sum_{j=1}^{n}\left[\eta_{\mathbf{e}_j}^{1/2}\,\rho_{\mathbf{s}}\,\eta_{\mathbf{e}_j}^{1/2} + \eta_{\mathbb{1}-\mathbf{e}_j}^{1/2}\,\rho_{\mathbf{s}}\,\eta_{\mathbb{1}-\mathbf{e}_j}^{1/2}\right]. \tag{27}$$

The previous definition is justified by the following result.

**Proposition 2.1** *$\mathcal{L}_{\mathbf{e}_1,\ldots,\mathbf{e}_n}$ is a unital rebit channel.*

*Proof.* To verify that $\mathcal{L}_{\mathbf{e}_1,\ldots,\mathbf{e}_n}$ is indeed a rebit channel it is enough to use the previously quoted Kraus decomposition theorem: $\mathcal{L}_{\mathbf{e}_1,\ldots,\mathbf{e}_n}$ is intrinsically defined in a Kraus form, so we just have to check that the constraint in eq. (18) is satisfied. Using the symmetry of $\eta_{\mathbf{e}_j}^{1/2}$ and $\eta_{\mathbb{1}-\mathbf{e}_j}^{1/2}$ for all $j = 1, \ldots, n$ and eq. (23), the Kraus constraint for $\mathcal{L}_{\mathbf{e}_1,\ldots,\mathbf{e}_n}$ becomes

$$\frac{1}{n}\sum_{j=1}^{n}\left(\eta_{\mathbf{e}_j}^{1/2}\eta_{\mathbf{e}_j}^{1/2} + \eta_{\mathbb{1}-\mathbf{e}_j}^{1/2}\eta_{\mathbb{1}-\mathbf{e}_j}^{1/2}\right) = \frac{1}{n}\sum_{j=1}^{n}\left(\eta_{\mathbf{e}_j} + \eta_{\mathbb{1}-\mathbf{e}_j}\right) = \frac{1}{n}\sum_{j=1}^{n}\left(\eta_{\mathbf{e}_j} + I_2 - \eta_{\mathbf{e}_j}\right) = I_2, \tag{28}$$

and so $\mathcal{L}_{\mathbf{e}_1,\ldots,\mathbf{e}_n}$ is indeed a rebit channel. Moreover, it can be verified by direct computation that $\mathcal{L}_{\mathbf{e}_1,\ldots,\mathbf{e}_n}(\rho_0) = \rho_0$, hence $\mathcal{L}_{\mathbf{e}_1,\ldots,\mathbf{e}_n}$ is unital. □

# 3 Action of $n$-Lüders channels on Bloch vectors

We can understand how $n$-Lüders channels modify a generic rebit state $\mathbf{s}$ by analyzing how they transform the associated Bloch vector $\mathbf{v}_{\mathbf{s}}$.

**Theorem 3.1** *A $n$-Lüders channel $\mathcal{L}_{\mathbf{e}_1,\ldots,\mathbf{e}_n}$ modifies the Bloch vector $\mathbf{v}_{\mathbf{s}}$ of a rebit state $\mathbf{s}$ as follows:*

$$\mathbf{v}_{\mathbf{s}} \underset{\mathcal{L}_{\mathbf{e}_1,\ldots,\mathbf{e}_n}}{\longmapsto} \mathbf{v}_{\mathcal{L}_{\mathbf{e}_1,\ldots,\mathbf{e}_n}(\mathbf{s})} = \frac{1}{n}\left[\left(\sum_{j=1}^{n}\alpha_{\mathbf{e}_j}\right)\mathbf{v}_{\mathbf{s}} + \sum_{j=1}^{n}\beta_{\mathbf{e}_j,\mathbf{s}}(1-\alpha_{\mathbf{e}_j})\mathbf{v}_{\mathbf{e}_j}\right], \tag{29}$$

*with $\alpha_{\mathbf{e}_j}$ and $\beta_{\mathbf{e}_j,\mathbf{s}}$ given by*

$$\alpha_{\mathbf{e}_j} := \|\mathbf{e}_j\|_{\mathcal{M}} + \|\mathbb{1} - \mathbf{e}_j\|_{\mathcal{M}} \qquad \textit{and} \qquad \beta_{\mathbf{e}_j,\mathbf{s}} := \frac{\mathbf{v}_{\mathbf{e}_j}\cdot\mathbf{v}_{\mathbf{s}}}{\|\mathbf{v}_{\mathbf{e}_j}\|^2}, \tag{30}$$

*where $\|\mathbf{e}_j\|_{\mathcal{M}} = \sqrt{(e_j)_0^2 - (e_j)_1^2 - (e_j)_2^2}$ and $\|\mathbb{1} - \mathbf{e}_j\|_{\mathcal{M}} = \sqrt{(1-(e_j)_0)^2 - (e_j)_1^2 - (e_j)_2^2}$ symbolize the 3D-Minkowski norm of $\mathbf{e}_j$ and $\mathbb{1} - \mathbf{e}_j$, for all $j = 1, \ldots, n$.*

*Proof.* By linearity and eq. (26) we have

$$\mathbf{v}_{\mathcal{L}_{\mathbf{e}_1,\ldots,\mathbf{e}_n}(\mathbf{s})} = \frac{1}{n}\sum_{j=1}^{n}\left[\mathbf{v}_{\psi_{\mathbf{e}_j}(\mathbf{s})} + \mathbf{v}_{\psi_{\mathbb{1}-\mathbf{e}_j}(\mathbf{s})}\right] = \frac{1}{n}\sum_{j=1}^{n}\mathbf{v}_{\mathcal{L}_{\mathbf{e}_j}(\mathbf{s})}, \tag{31}$$

where

$$\mathbf{v}_{\mathcal{L}_{\mathbf{e}_j}(\mathbf{s})} = \mathbf{v}_{\psi_{\mathbf{e}_j}(\mathbf{s})} + \mathbf{v}_{\psi_{\mathbb{1}-\mathbf{e}_j}(\mathbf{s})}, \tag{32}$$

and $\mathbf{v}_{\psi_{\mathbf{e}_j}(\mathbf{s})}$ and $\mathbf{v}_{\psi_{\mathbb{1}-\mathbf{e}_j}}(\mathbf{s})$ are defined as in eq. (15) replacing $\mathbf{e}$ by $\mathbf{e}_j$ and $\mathbb{1}-\mathbf{e}_j$, respectively. So, it is enough to study the vector $\mathbf{v}_{\mathcal{L}_{\mathbf{e}_j}(\mathbf{s})}$ with $j$ fixed and then sum the contributions as $j$ runs over the index set. To make the following formulae more easily readable, we will momentarily drop the suffix $j$ and restore it only at the end of our computations.

With this simplification in mind, we can rewrite the last equation as $\mathbf{v}_{\mathcal{L}_{\mathbf{e}}(\mathbf{s})} = \mathbf{v}_{\psi_{\mathbf{e}}(\mathbf{s})} + \mathbf{v}_{\psi_{\mathbb{1}-\mathbf{e}}(\mathbf{s})}$ and make the vectors appearing on the right-hand side explicit:

$$\mathbf{v}_{\psi_{\mathbf{e}}(\mathbf{s})} = \mathrm{Tr}(\psi_{\mathbf{e}}(\mathbf{s}))\mathbf{v}_{\mathbf{e}} \oplus \mathbf{v}_{\mathbf{s}} = \mathrm{Tr}(\rho_{\mathbf{s}}\eta_{\mathbf{e}})\mathbf{v}_{\mathbf{e}} \oplus \mathbf{v}_{\mathbf{s}} = e_0(1+\mathbf{v}_{\mathbf{e}}\cdot\mathbf{v}_{\mathbf{s}})\mathbf{v}_{\mathbf{e}} \oplus \mathbf{v}_{\mathbf{s}}, \tag{33}$$

$$\begin{aligned}\mathbf{v}_{\psi_{\mathbb{1}-\mathbf{e}}(\mathbf{s})} &= \mathrm{Tr}(\psi_{\mathbb{1}-\mathbf{e}}(\mathbf{s}))\mathbf{v}_{\mathbb{1}-\mathbf{e}} \oplus \mathbf{v}_{\mathbf{s}} = \mathrm{Tr}(\rho_{\mathbf{s}}(I_2-\eta_{\mathbf{e}}))\mathbf{v}_{\mathbb{1}-\mathbf{e}} \oplus \mathbf{v}_{\mathbf{s}} \\ &= [\mathrm{Tr}(\rho_{\mathbf{s}}) - \mathrm{Tr}(\rho_{\mathbf{s}}\eta_{\mathbf{e}})]\mathbf{v}_{\mathbb{1}-\mathbf{e}} \oplus \mathbf{v}_{\mathbf{s}} = [1-e_0(1+\mathbf{v}_{\mathbf{e}}\cdot\mathbf{v}_{\mathbf{s}})]\,\mathbf{v}_{\mathbb{1}-\mathbf{e}} \oplus \mathbf{v}_{\mathbf{s}}\end{aligned} \tag{34}$$

but, using eq. (24), we have

$$1+\mathbf{v}_{\mathbb{1}-\mathbf{e}}\cdot\mathbf{v}_{\mathbf{s}} = 1-\frac{e_0}{1-e_0}\mathbf{v}_{\mathbf{e}}\cdot\mathbf{v}_{\mathbf{s}} = \frac{1-e_0(1+\mathbf{v}_{\mathbf{e}}\cdot\mathbf{v}_{\mathbf{s}})}{1-e_0}, \tag{35}$$

so

$$\mathbf{v}_{\psi_{\mathbb{1}-\mathbf{e}}(\mathbf{s})} = (1-e_0)(1+\mathbf{v}_{\mathbb{1}-\mathbf{e}}\cdot\mathbf{v}_{\mathbf{s}})\mathbf{v}_{\mathbb{1}-\mathbf{e}} \oplus \mathbf{v}_{\mathbf{s}} \tag{36}$$

and thus

$$\mathbf{v}_{\mathcal{L}_{\mathbf{e}}(\mathbf{s})} = e_0(1+\mathbf{v}_{\mathbf{e}}\cdot\mathbf{v}_{\mathbf{s}})\mathbf{v}_{\mathbf{e}} \oplus \mathbf{v}_{\mathbf{s}} + (1-e_0)(1+\mathbf{v}_{\mathbb{1}-\mathbf{e}}\cdot\mathbf{v}_{\mathbf{s}})\mathbf{v}_{\mathbb{1}-\mathbf{e}} \oplus \mathbf{v}_{\mathbf{s}}. \tag{37}$$

By making explicit the expression of the Einstein-Poincaré relativistic sum recalled in eq. (12) we find

$$\begin{aligned}\mathbf{v}_{\mathcal{L}_{\mathbf{e}}(\mathbf{s})} &= e_0\left\{\mathbf{v}_{\mathbf{e}} + \frac{1}{\gamma_{\mathbf{v}_{\mathbf{e}}}}\mathbf{v}_{\mathbf{s}} + \frac{\gamma_{\mathbf{v}_{\mathbf{e}}}}{1+\gamma_{\mathbf{v}_{\mathbf{e}}}}(\mathbf{v}_{\mathbf{e}}\cdot\mathbf{v}_{\mathbf{s}})\mathbf{v}_{\mathbf{e}}\right\} \\ &\quad + (1-e_0)\left\{\mathbf{v}_{\mathbb{1}-\mathbf{e}} + \frac{1}{\gamma_{\mathbf{v}_{\mathbb{1}-\mathbf{e}}}}\mathbf{v}_{\mathbf{s}} + \frac{\gamma_{\mathbf{v}_{\mathbb{1}-\mathbf{e}}}}{1+\gamma_{\mathbf{v}_{\mathbb{1}-\mathbf{e}}}}(\mathbf{v}_{\mathbb{1}-\mathbf{e}}\cdot\mathbf{v}_{\mathbf{s}})\mathbf{v}_{\mathbb{1}-\mathbf{e}}\right\} \\ &= e_0\left\{\mathbf{v}_{\mathbf{e}} + \frac{1}{\gamma_{\mathbf{v}_{\mathbf{e}}}}\mathbf{v}_{\mathbf{s}} + \frac{\gamma_{\mathbf{v}_{\mathbf{e}}}}{1+\gamma_{\mathbf{v}_{\mathbf{e}}}}(\mathbf{v}_{\mathbf{e}}\cdot\mathbf{v}_{\mathbf{s}})\mathbf{v}_{\mathbf{e}}\right\} \\ &\quad + (1-e_0)\left\{-\frac{e_0}{1-e_0}\mathbf{v}_{\mathbf{e}} + \frac{1}{\gamma_{\mathbf{v}_{\mathbb{1}-\mathbf{e}}}}\mathbf{v}_{\mathbf{s}} + \frac{e_0^2}{(1-e_0)^2}\frac{\gamma_{\mathbf{v}_{\mathbb{1}-\mathbf{e}}}}{1+\gamma_{\mathbf{v}_{\mathbb{1}-\mathbf{e}}}}(\mathbf{v}_{\mathbf{e}}\cdot\mathbf{v}_{\mathbf{s}})\mathbf{v}_{\mathbf{e}}\right\},\end{aligned} \tag{38}$$

where the Lorentz factors relative to the vectors $\mathbf{v}_{\mathbf{e}}$ and $\mathbf{v}_{\mathbb{1}-\mathbf{e}}$ are

$$\gamma_{\mathbf{v}_{\mathbf{e}}} = \frac{e_0}{\sqrt{e_0^2-e_1^2-e_2^2}} = \frac{e_0}{\|\mathbf{e}\|_{\mathcal{M}}} \quad \text{and} \quad \gamma_{\mathbf{v}_{\mathbb{1}-\mathbf{e}}} = \frac{1-e_0}{\sqrt{(1-e_0)^2-e_1^2-e_2^2}} = \frac{1-e_0}{\|\mathbb{1}-\mathbf{e}\|_{\mathcal{M}}}, \tag{39}$$

so that

$$\frac{\gamma_{\mathbf{v}_{\mathbf{e}}}}{1+\gamma_{\mathbf{v}_{\mathbf{e}}}} = \frac{e_0}{e_0+\|\mathbf{e}\|_{\mathcal{M}}} \quad \text{and} \quad \frac{\gamma_{\mathbf{v}_{\mathbb{1}-\mathbf{e}}}}{1+\gamma_{\mathbf{v}_{\mathbb{1}-\mathbf{e}}}} = \frac{1-e_0}{1-e_0+\|\mathbb{1}-\mathbf{e}\|_{\mathcal{M}}}. \tag{40}$$

It follows that

$$\begin{aligned}\mathbf{v}_{\mathcal{L}_{\mathbf{e}}(\mathbf{s})} &= \|\mathbf{e}\|_{\mathcal{M}}\mathbf{v}_{\mathbf{s}} + \frac{e_0^2}{e_0+\|\mathbf{e}\|_{\mathcal{M}}}(\mathbf{v}_{\mathbf{e}}\cdot\mathbf{v}_{\mathbf{s}})\mathbf{v}_{\mathbf{e}} + \|\mathbb{1}-\mathbf{e}\|_{\mathcal{M}}\mathbf{v}_{\mathbf{s}} + \frac{e_0^2}{1-e_0+\|\mathbb{1}-\mathbf{e}\|_{\mathcal{M}}}(\mathbf{v}_{\mathbf{e}}\cdot\mathbf{v}_{\mathbf{s}})\mathbf{v}_{\mathbf{e}} \\ &= (\|\mathbf{e}\|_{\mathcal{M}}+\|\mathbb{1}-\mathbf{e}\|_{\mathcal{M}})\mathbf{v}_{\mathbf{s}} + e_0^2(\mathbf{v}_{\mathbf{e}}\cdot\mathbf{v}_{\mathbf{s}})\left(\frac{1}{e_0+\|\mathbf{e}\|_{\mathcal{M}}} + \frac{1}{1-e_0+\|\mathbb{1}-\mathbf{e}\|_{\mathcal{M}}}\right)\mathbf{v}_{\mathbf{e}} \\ &= (\|\mathbf{e}\|_{\mathcal{M}}+\|\mathbb{1}-\mathbf{e}\|_{\mathcal{M}})\mathbf{v}_{\mathbf{s}} + e_0^2(\mathbf{v}_{\mathbf{e}}\cdot\mathbf{v}_{\mathbf{s}})\left(\frac{e_0-\|\mathbf{e}\|_{\mathcal{M}}}{e_1^2+e_2^2} + \frac{1-e_0-\|\mathbb{1}-\mathbf{e}\|_{\mathcal{M}}}{e_1^2+e_2^2}\right)\mathbf{v}_{\mathbf{e}} \\ &= (\|\mathbf{e}\|_{\mathcal{M}}+\|\mathbb{1}-\mathbf{e}\|_{\mathcal{M}})\mathbf{v}_{\mathbf{s}} + \frac{\mathbf{v}_{\mathbf{e}}\cdot\mathbf{v}_{\mathbf{s}}}{\|\mathbf{v}_{\mathbf{e}}\|^2}(1-\|\mathbf{e}\|_{\mathcal{M}}-\|\mathbb{1}-\mathbf{e}\|_{\mathcal{M}})\mathbf{v}_{\mathbf{e}},\end{aligned} \tag{41}$$

having used in the last step the fact that $e_1^2/e_0^2 + e_2^2/e_0^2 = \|\mathbf{v_e}\|^2$.

Now, reintroducing the suffix $j$ and using eq. (30) we find

$$\mathbf{v}_{\mathcal{L}_{\mathbf{e}_j}(\mathbf{s})} = \alpha_{\mathbf{e}_j}\mathbf{v_s} + \beta_{\mathbf{e}_j,\mathbf{s}}(1-\alpha_{\mathbf{e}_j})\mathbf{v}_{\mathbf{e}_j}, \tag{42}$$

and so eq. (31) leads directly to formula (29). □

It is worthwhile to single out some noticeable values of $\alpha_{\mathbf{e}}$ and $\beta_{\mathbf{e},\mathbf{s}}$. First of all, the conditions defining the effect space $\mathcal{E}$ guarantee that $\alpha_{\mathbf{e}}$ is the sum of real square roots, hence $\alpha_{\mathbf{e}} \geq 0$.

The largest value that $\alpha_{\mathbf{e}}$ can reach corresponds clearly to the condition $e_1 = e_2 = 0$, in which case $\alpha_{\mathbf{e}} = 1$.

On the contrary, both terms appearing in $\alpha_{\mathbf{e}}$ are null only for effects belonging to the circumference of the disk that lies at the basis of $\mathcal{E}$. These effects are characterized by $e_0 = 1/2$ and $e_1^2 + e_2^2 = 1/4$, which imply $\|\mathbf{v_e}\| = 1$.

To resume, for all $\mathbf{e} \in \mathcal{E}$, $\alpha_{\mathbf{e}} \in [0,1]$ and

$$\alpha_{\mathbf{e}} = 1 \iff \mathbf{v_e} = \mathbf{0} \quad \forall e_0 \in (0,1), \tag{43}$$

while

$$\alpha_{\mathbf{e}} = 0 \iff \|\mathbf{v_e}\| = 1 \text{ and } e_0 = \frac{1}{2}. \tag{44}$$

It will be useful to characterize effects satisfying eqs. (43) and (44) with special names:

- $\mathbf{e} \in \mathcal{E}$ is *neutral* if it satisfies eq. (43);
- $\mathbf{e} \in \mathcal{E}$ is *extremal* if it satisfies eq. (44).

Neutral and extremal effects are visualized on the double cone of the effect space in Figure 3 and 4, respectively.

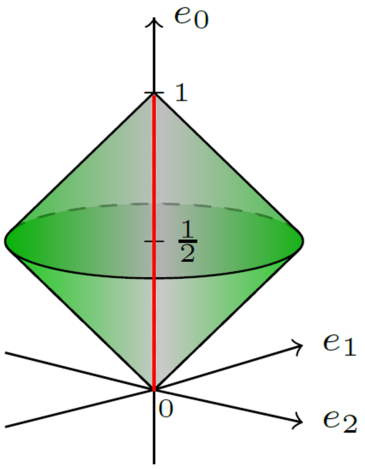


Figure 3: Neutral effects $\mathbf{e}$ lie on the vertical axis (without vertices) of the effect space $\mathcal{E}$.

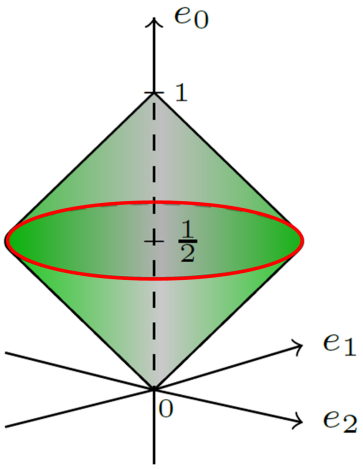


Figure 4: Extremal effects $\mathbf{e}$ lie on the base circle of the effect space $\mathcal{E}$ at height 1/2.

Regarding $\beta_{\mathbf{e},\mathbf{s}}$ we have:

- $\beta_{\mathbf{e},\mathbf{s}} \in [-1,1]$, with extremes reached when $\mathbf{v_s} = -\mathbf{v_e}$ and $\mathbf{v_s} = \mathbf{v_e}$, respectively;
- $\beta_{\mathbf{e},\mathbf{s}} = 0$ if and only if $\mathbf{v_e}$ and $\mathbf{v_s}$ are orthogonal.

# 4 Rebit channels that can be expressed as $n$-Lüders channels

The analysis of eq. (29) in polar coordinates will allow us understanding what type of rebit channels can be represented by $n$-Lüders channels.

For this, we write the $n$ effect vectors as follows

$$\mathbf{v}_{\mathbf{e}_j} = r_{\mathbf{e}_j} \begin{pmatrix} \cos\vartheta_{\mathbf{e}_j} \\ \sin\vartheta_{\mathbf{e}_j} \end{pmatrix}, \tag{45}$$

where $\vartheta_{\mathbf{e}_j}$ is the angle between $\mathbf{v}_{\mathbf{e}_j}$ and the horizontal axis of the Bloch disk. Then,

$$\beta_{\mathbf{e}_j,\mathbf{s}}\mathbf{v}_{\mathbf{e}_j} = r_{\mathbf{s}} \cos\vartheta_{\mathbf{e}_j,\mathbf{s}} \begin{pmatrix} \cos\vartheta_{\mathbf{e}_j} \\ \sin\vartheta_{\mathbf{e}_j} \end{pmatrix}, \tag{46}$$

where $\vartheta_{\mathbf{e}_j,\mathbf{s}} = \vartheta_{\mathbf{s}} - \vartheta_{\mathbf{e}_j}$ is the angle between $\mathbf{v}_{\mathbf{s}}$ and $\mathbf{v}_{\mathbf{e}_j}$, so $\cos\vartheta_{\mathbf{e}_j,\mathbf{s}} = \cos\vartheta_{\mathbf{s}}\cos\vartheta_{\mathbf{e}_j} + \sin\vartheta_{\mathbf{s}}\sin\vartheta_{\mathbf{e}_j}$ and

$$\beta_{\mathbf{e}_j,\mathbf{s}}\mathbf{v}_{\mathbf{e}_j} = r_s \begin{pmatrix} \cos\vartheta_{\mathbf{s}}\cos^2\vartheta_{\mathbf{e}_j} + \sin\vartheta_{\mathbf{s}}\cos\vartheta_{\mathbf{e}_j}\sin\vartheta_{\mathbf{e}_j} \\ \sin\vartheta_{\mathbf{s}}\sin^2\vartheta_{\mathbf{e}_j} + \cos\vartheta_{\mathbf{s}}\cos\vartheta_{\mathbf{e}_j}\sin\vartheta_{\mathbf{e}_j} \end{pmatrix} = r_{\mathbf{s}} \begin{pmatrix} \cos\vartheta_{\mathbf{s}}\cos^2\vartheta_{\mathbf{e}_j} + \frac{1}{2}\sin\vartheta_{\mathbf{s}}\sin(2\vartheta_{\mathbf{e}_j}) \\ \sin\vartheta_{\mathbf{s}}\sin^2\vartheta_{\mathbf{e}_j} + \frac{1}{2}\cos\vartheta_{\mathbf{s}}\sin(2\vartheta_{\mathbf{e}_j}) \end{pmatrix}. \tag{47}$$

Thanks to these computations, the generic expression of eq. (29) in polar coordinates can be written as follows

$$\mathbf{v}_{\mathcal{L}_{\mathbf{e}_1,\ldots,\mathbf{e}_n}(\mathbf{s})} = r_{\mathbf{s}} \begin{pmatrix} a_{\mathbf{e}_1,\ldots,\mathbf{e}_n}\cos\vartheta_{\mathbf{s}} + b_{\mathbf{e}_1,\ldots,\mathbf{e}_n}\sin\vartheta_{\mathbf{s}} \\ b_{\mathbf{e}_1,\ldots,\mathbf{e}_n}\cos\vartheta_{\mathbf{s}} + c_{\mathbf{e}_1,\ldots,\mathbf{e}_n}\sin\vartheta_{\mathbf{s}} \end{pmatrix}, \tag{48}$$

where

$$\begin{cases} a_{\mathbf{e}_1,\ldots,\mathbf{e}_n} := \dfrac{1}{n}\displaystyle\sum_{j=1}^{n}\left(\alpha_{\mathbf{e}_j} + (1-\alpha_{\mathbf{e}_j})\cos^2\vartheta_{\mathbf{e}_j}\right) & (49) \\ b_{\mathbf{e}_1,\ldots,\mathbf{e}_n} := \dfrac{1}{2n}\displaystyle\sum_{j=1}^{n}(1-\alpha_{\mathbf{e}_j})\sin(2\vartheta_{\mathbf{e}_j}) & (50) \\ c_{\mathbf{e}_1,\ldots,\mathbf{e}_n} := \dfrac{1}{n}\displaystyle\sum_{j=1}^{n}\left(\alpha_{\mathbf{e}_j} + (1-\alpha_{\mathbf{e}_j})\sin^2\vartheta_{\mathbf{e}_j}\right) & (51) \end{cases}.$$

In the following list, we study eq. (48) in full detail.

1. First of all we, notice that $\mathcal{L}_{\mathbf{e}_1,\ldots,\mathbf{e}_n}$ *is the identity channel if and only if all the effects* $\mathbf{e}_1,\ldots,\mathbf{e}_n$ *are neutral*. In fact the identity equation written for Bloch vectors, i.e.

$$\mathbf{v}_{\mathcal{L}_{\mathbf{e}_1,\ldots,\mathbf{e}_n}(\mathbf{s})} = r_{\mathbf{s}} \begin{pmatrix} \cos\vartheta_{\mathbf{s}} \\ \sin\vartheta_{\mathbf{s}} \end{pmatrix} = \mathbf{v}_{\mathbf{s}} \tag{52}$$

   is satisfied if and only if $a_{\mathbf{e}_1,\ldots,\mathbf{e}_n} = c_{\mathbf{e}_1,\ldots,\mathbf{e}_n} = 1$ and $b_{\mathbf{e}_1,\ldots,\mathbf{e}_n} = 0$. This can only happen when $\alpha_{\mathbf{e}_j} = 1$ for all $j = 1,\ldots,n$, which is precisely the condition that defines the neutrality of all the effects $\mathbf{e}_1,\ldots,\mathbf{e}_n$.

2. The coefficients $a_{\mathbf{e}_1,\ldots,\mathbf{e}_n}$ and $c_{\mathbf{e}_1,\ldots,\mathbf{e}_n}$ are sums of non-negative terms, hence they cannot be simultaneously null due to the presence of $\cos^2(\vartheta_{\mathbf{e}_j})$ and $\sin^2(\vartheta_{\mathbf{e}_j})$, which can never be nullified at the same time. The only way of canceling out $\cos^2(\vartheta_{\mathbf{e}_j})$ and $\sin^2(\vartheta_{\mathbf{e}_j})$ is to set $\alpha_{\mathbf{e}_j} = 1$ for all $j = 1,\ldots,n$, which leads the the identity channel, as we have just proven. As a consequence, the $n$-Lüders channels do not exhaust all rebit channels because they cannot represent the complete state space contraction, i.e. the channel which transforms all the states into the maximally mixed state $\rho_0$ or, equivalently, that nullifies all the Bloch vectors. Hence, there exists a strictly positive lower bound to the shrinking ability of the Bloch disk by $\mathcal{L}_{\mathbf{e}_1,\ldots,\mathbf{e}_n}$ and no $n$-Lüders channel can represent a rebit channel which shrinks the Bloch disk more than that.

3. If $b_{\mathbf{e}_1,\ldots,\mathbf{e}_n} = 0$ and $a_{\mathbf{e}_1,\ldots,\mathbf{e}_n}, c_{\mathbf{e}_1,\ldots,\mathbf{e}_n} \neq 0$, then eq. (48) becomes

$$\mathbf{v}_{\mathcal{L}_{\mathbf{e}_1,\ldots,\mathbf{e}_n}(\mathbf{s})} = r_{\mathbf{s}} \begin{pmatrix} a_{\mathbf{e}_1,\ldots,\mathbf{e}_n} \cos\vartheta_{\mathbf{s}} \\ c_{\mathbf{e}_1,\ldots,\mathbf{e}_n} \sin\vartheta_{\mathbf{s}} \end{pmatrix}, \tag{53}$$

the coordinates of $\mathbf{v}_{\mathcal{L}_{\mathbf{e}_1,\ldots,\mathbf{e}_n}(\mathbf{s})}$ in this case describe an ellipse centered at the origin, oriented as the Cartesian axes and with semi-axes lengths given by $a_{\mathbf{e}_1,\ldots,\mathbf{e}_n}$ and $c_{\mathbf{e}_1,\ldots,\mathbf{e}_n}$, i.e. *a generic phase-flip channel*. If $a_{\mathbf{e}_1,\ldots,\mathbf{e}_n} = 1$ or $c_{\mathbf{e}_1,\ldots,\mathbf{e}_n} = 1$, $\mathcal{L}_{\mathbf{e}_1,\ldots,\mathbf{e}_n}$ behaves as *a phase-flip channel of the type* $(1, 1-p)$ or $(1-p, 1)$, with $p \in (0,1)$. Finally, if $a_{\mathbf{e}_1,\ldots,\mathbf{e}_n} = c_{\mathbf{e}_1,\ldots,\mathbf{e}_n} \equiv R$, the ellipse becomes a circle with radius $R$ and $\mathcal{L}_{\mathbf{e}_1,\ldots,\mathbf{e}_n}$ behaves as *a depolarizing channel*.

4. If $a_{\mathbf{e}_1,\ldots,\mathbf{e}_n} = b_{\mathbf{e}_1,\ldots,\mathbf{e}_n} = 0$, but $c_{\mathbf{e}_1,\ldots,\mathbf{e}_n} \neq 0$ (respectively, $b_{\mathbf{e}_1,\ldots,\mathbf{e}_n} = c_{\mathbf{e}_1,\ldots,\mathbf{e}_n} = 0$, but $a_{\mathbf{e}_1,\ldots,\mathbf{e}_n} \neq 0$), then, as $\vartheta_{\mathbf{s}}$ varies in $[0, 2\pi)$, the coordinates of $\mathbf{v}_{\mathcal{L}_{\mathbf{e}_1,\ldots,\mathbf{e}_n}(\mathbf{s})}$ in eq. (48) lie on a vertical (respectively, horizontal) segment of half length $c_{\mathbf{e}_1,\ldots,\mathbf{e}_n}$ (respectively, $a_{\mathbf{e}_1,\ldots,\mathbf{e}_n}$). In these cases, $\mathcal{L}_{\mathbf{e}_1,\ldots,\mathbf{e}_n}$ behaves as a *linear channel*. Actually, it cannot be a generic linear channel, but it coincides with *a degenerate phase-flip channel of type* $(1,0)$ *or* $(0,1)$, because the only way of nullifying $a_{\mathbf{e}_1,\ldots,\mathbf{e}_n}$ and $b_{\mathbf{e}_1,\ldots,\mathbf{e}_n}$ simultaneously is to impose $\alpha_{\mathbf{e}_j} = 0$ and $\vartheta_{\mathbf{e}_j} = \pi/2$ or $\vartheta_{\mathbf{e}_j} = 3\pi/2$ for all $j = 1, \ldots, n$, which imply $c_{\mathbf{e}_1,\ldots,\mathbf{e}_n} = 1$. Analogously, $b_{\mathbf{e}_1,\ldots,\mathbf{e}_n}$ and $c_{\mathbf{e}_1,\ldots,\mathbf{e}_n}$ are simultaneously null if and only if $\alpha_{\mathbf{e}_j} = 0$ and $\vartheta_{\mathbf{e}_j} = 0$ or $\vartheta_{\mathbf{e}_j} = \pi$ for all $j = 1, \ldots, n$, which imply $a_{\mathbf{e}_1,\ldots,\mathbf{e}_n} = 1$.

5. More generally, if $b_{\mathbf{e}_1,\ldots,\mathbf{e}_n} \neq 0$, the coordinates of $\mathbf{v}_{\mathcal{L}_{\mathbf{e}_1,\ldots,\mathbf{e}_n}(\mathbf{s})}$ in eq. (48) describe the points of the *Lissajous curve*

$$\begin{aligned} \vec{\mathcal{L}}_{\mathbf{e}_1,\ldots,\mathbf{e}_n} : \quad [0,2\pi) \quad &\longrightarrow \quad \mathcal{D} \subset \mathbb{R}^2 \\ \vartheta_{\mathbf{s}} \quad &\longmapsto \quad \vec{\mathcal{L}}_{\mathbf{s},\mathbf{e}_1,\ldots,\mathbf{e}_n}(\vartheta_{\mathbf{s}}) := \mathbf{v}_{\mathcal{L}_{\mathbf{e}_1,\ldots,\mathbf{e}_n}(\mathbf{s})} = r_{\mathbf{s}} \begin{pmatrix} R^{(1)}_{\mathbf{e}_1,\ldots,\mathbf{e}_n} \sin(\vartheta_{\mathbf{s}} + \phi^{(1)}_{\mathbf{e}_1,\ldots,\mathbf{e}_n}) \\ R^{(2)}_{\mathbf{e}_1,\ldots,\mathbf{e}_n} \sin(\vartheta_{\mathbf{s}} + \phi^{(2)}_{\mathbf{e}_1,\ldots,\mathbf{e}_n}) \end{pmatrix}, \end{aligned} \tag{54}$$

where

$$R^{(1)}_{\mathbf{e}_1,\ldots,\mathbf{e}_n} := \sqrt{a^2_{\mathbf{e}_1,\ldots,\mathbf{e}_n} + b^2_{\mathbf{e}_1,\ldots,\mathbf{e}_n}}, \tag{55}$$

$$R^{(2)}_{\mathbf{e}_1,\ldots,\mathbf{e}_n} := \sqrt{c^2_{\mathbf{e}_1,\ldots,\mathbf{e}_n} + b^2_{\mathbf{e}_1,\ldots,\mathbf{e}_n}}, \tag{56}$$

$$\phi^{(1)}_{\mathbf{e}_1,\ldots,\mathbf{e}_n} := \begin{cases} \arctan\left(\frac{b_{\mathbf{e}_1,\ldots,\mathbf{e}_n}}{a_{\mathbf{e}_1,\ldots,\mathbf{e}_n}}\right) & \text{if } a_{\mathbf{e}_1,\ldots,\mathbf{e}_n} \neq 0 \\ 0 & \text{otherwise} \end{cases}, \tag{57}$$

$$\phi^{(2)}_{\mathbf{e}_1,\ldots,\mathbf{e}_n} := \arctan\left(\frac{c_{\mathbf{e}_1,\ldots,\mathbf{e}_n}}{b_{\mathbf{e}_1,\ldots,\mathbf{e}_n}}\right). \tag{58}$$

Since $\vartheta_{\mathbf{s}}$ appears multiplied by the same coefficient in both coordinates, the points of the Lissajous curve $\vec{\mathcal{L}}_{\mathbf{e}_1,\ldots,\mathbf{e}_n}$ lie on an ellipse centered at the origin, coherently with the classification of unital rebit channels. This ellipse is tilted with respect to the Cartesian axes.

6. If $b_{\mathbf{e}_1,\ldots,\mathbf{e}_n} \neq 0$ and $\alpha_{\mathbf{e}_j} = 0$ for all $j = 1, \ldots, n$, i.e. when all the effects $\mathbf{e}_1, \ldots, \mathbf{e}_n$ are extremal, eqs. (55) and (56) give

$$R^{(1)}_{\mathbf{e}_1,\ldots,\mathbf{e}_n} = \frac{1}{n}\sqrt{\left(\sum_{j=1}^{n} \cos^2\vartheta_{\mathbf{e}_j}\right)^2 + \frac{1}{4}\left(\sum_{j=1}^{n} \sin(2\vartheta_{\mathbf{e}_j})\right)^2}, \tag{59}$$

$$R^{(2)}_{\mathbf{e}_1,\ldots,\mathbf{e}_n} = \frac{1}{n}\sqrt{\left(\sum_{j=1}^{n} \sin^2\vartheta_{\mathbf{e}_j}\right)^2 + \frac{1}{4}\left(\sum_{j=1}^{n} \sin(2\vartheta_{\mathbf{e}_j})\right)^2}. \tag{60}$$

There are multiple ways to obtain a depolarizing channel in this case. Hereby we examine two simple ones.

- If the effects $\mathbf{e}_1, \ldots, \mathbf{e}_n$ are such that $\vartheta_{\mathbf{e}_j} = \pi/4 + k\pi/2$, $k \in \{1, 2, 3\}$, then we get $\cos^2 \vartheta_{\mathbf{e}_j} = \sin^2 \vartheta_{\mathbf{e}_j} = 1/2$ for all $j = 1, \ldots, n$ and, by direct computation, we find that $\mathcal{L}_{\mathbf{e}_1,\ldots,\mathbf{e}_n}$ shrinks the Bloch disk to another disk[2] of radius $R = \sqrt{3}/2$.
- If $n \geq 2$ is *even*, a general strategy to build depolarizing channels is to consider couples of effects $(\mathbf{e}_i, \mathbf{e}_k)$, $i, k \in \{1, \ldots, n\}$, $i \neq k$, with orthogonal vectors $\mathbf{v}_{\mathbf{e}_i} \perp \mathbf{v}_{\mathbf{e}_k}$, i.e. $|\vartheta_{\mathbf{e}_i} - \vartheta_{\mathbf{e}_k}| = \pi/2$. In fact, in this case we have

$$\sin(2\vartheta_{\mathbf{e}_i}) = \sin(2(\vartheta_{\mathbf{e}_k} \pm \pi/2)) = \sin(2\vartheta_{\mathbf{e}_k} \pm \pi) = -\sin(2\vartheta_{\mathbf{e}_k}), \tag{61}$$

so $\sum_{j=1}^{n} \sin(2\vartheta_{\mathbf{e}_j}) = 0$ and we remain with

$$R^{(1)}_{\mathbf{e}_1,\ldots,\mathbf{e}_n} = \frac{1}{n} \sum_{j=1}^{n} \cos^2 \vartheta_{\mathbf{e}_j}, \quad R^{(2)}_{\mathbf{e}_1,\ldots,\mathbf{e}_n} = \frac{1}{n} \sum_{j=1}^{n} \sin^2 \vartheta_{\mathbf{e}_j}, \tag{62}$$

moreover, $\cos^2 \vartheta_{\mathbf{e}_i} + \cos^2 \vartheta_{\mathbf{e}_k} = \cos^2(\vartheta_{\mathbf{e}_k} \pm \pi/2) + \cos^2 \vartheta_{\mathbf{e}_k} = \sin^2 \vartheta_{\mathbf{e}_k} + \cos^2 \vartheta_{\mathbf{e}_k} = 1$ and, analogously, $\sin^2 \vartheta_{\mathbf{e}_i} + \sin^2 \vartheta_{\mathbf{e}_k} = 1$ for all couples of effects with orthogonal vectors. Since there are precisely $n/2$ couples, we obtain $R^{(1)}_{\mathbf{e}_1,\ldots,\mathbf{e}_n} = R^{(2)}_{\mathbf{e}_1,\ldots,\mathbf{e}_n} = 1/2$ and so $\mathcal{L}_{\mathbf{e}_1,\ldots,\mathbf{e}_n}$ shrinks the Bloch disk to another disk of radius $1/2$.

7. Finally, if $b_{\mathbf{e}_1,\ldots,\mathbf{e}_n} \neq 0$ but the coefficients $\alpha_{\mathbf{e}_j}$ are not necessarily all null, we can obtain interesting iterative formulae for eq. (48) by considering the following conditions

$$\begin{cases} \vartheta_{\mathbf{e}_1} = k\frac{\pi}{2} & k \in \{0, 1, 2, 3\} \\ \mathbf{v}_{\mathbf{e}_j} \perp \mathbf{v}_{\mathbf{e}_{j+1}} & \forall j = 1, \ldots, n-1 \\ \mathbf{v}_{\mathbf{e}_j} \parallel \mathbf{v}_{\mathbf{e}_{j+2}} & \forall j = 1, \ldots, n-2 \end{cases}. \tag{63}$$

When $n$ is even, say $n = 2m$, with $m \in \mathbb{N}$, $m \geq 2$, we get:

$$\mathbf{v}_{\mathcal{L}_{\mathbf{e}_1,\ldots,\mathbf{e}_{2m}}(\mathbf{s})} = \frac{1}{2} \begin{pmatrix} \left(1 + \frac{1}{m} \sum_{k=1}^{m} \alpha_{\mathbf{e}_{2k}}\right) r_{\mathbf{s}} \cos \vartheta_{\mathbf{s}} \\ \left(1 + \frac{1}{m} \sum_{\ell=0}^{m-1} \alpha_{\mathbf{e}_{2\ell+1}}\right) r_{\mathbf{s}} \sin \vartheta_{\mathbf{s}} \end{pmatrix}. \tag{64}$$

When $n$ is odd, say $n = 2m + 1$, with $m \in \mathbb{N}$, $m \geq 1$, we get:

$$\mathbf{v}_{\mathcal{L}_{\mathbf{e}_1,\ldots,\mathbf{e}_{2m+1}}(\mathbf{s})} = \frac{1}{2m+1} \begin{pmatrix} \left(m + 1 + \sum_{k=1}^{m} \alpha_{\mathbf{e}_{2k}}\right) r_{\mathbf{s}} \cos \vartheta_{\mathbf{s}} \\ \left(m + \sum_{\ell=0}^{m} \alpha_{\mathbf{e}_{2\ell+1}}\right) r_{\mathbf{s}} \sin \vartheta_{\mathbf{s}} \end{pmatrix}. \tag{65}$$

Notice that, in this case, one of the two semi-axes of the ellipses into which the Bloch disk is shrunk can be smaller than $1/2$, but not the other. The smallest length is $1/3$ and it is achieved in the case $n = 3$. As $n$ grows, the minimal semi-axis length approaches $1/2$.

In the following subsections, we analyze the special cases of 1-Lüders and 2-Lüders channels.

## 4.1 1-Lüders channels

In the special case of 1-Lüders channels, modulo a rotation, it is always possible to consider the coordinate system in which the angles are measured with respect to the direction defined by $\mathbf{v}_{\mathbf{e}}$. So $\vartheta_{\mathbf{e}} = 0$ and $b_{\mathbf{e}} = 0$, thus eq. (48) reduces to eq. (53) with $a_{\mathbf{e}} = 1$ and $c_{\mathbf{e}} = \alpha_{\mathbf{e}}$, i.e.

$$\mathbf{v}_{\mathcal{L}_{\mathbf{e}}(\mathbf{s})} = \begin{pmatrix} r_{\mathbf{s}} \cos \vartheta_{\mathbf{s}} \\ \alpha_{\mathbf{e}} r_{\mathbf{s}} \sin \vartheta_{\mathbf{s}} \end{pmatrix}, \tag{66}$$

[2]We recall that eqs. (59) and (60) hold under the hypothesis that $b_{\mathbf{e}_1,\ldots,\mathbf{e}_n} \neq 0$. As we will see in subsection 4.1, when $n = 1$ the coefficient $b$ can always be considered null, hence this result is valid only for $n \geq 2$.

which means that the component of $\mathbf{v_s}$ collinear with $\mathbf{v_e}$ is left fixed by $\mathcal{L}_\mathbf{e}$, while the orthogonal one is shrunk by the quantity $\alpha_\mathbf{e}$, so, in particular

$$\mathbf{v}_{\mathcal{L}_\mathbf{e}(\mathbf{s})} = \begin{cases} \mathbf{v_s} & \text{if } \mathbf{v_s} \parallel \mathbf{v_e} \\ \alpha_\mathbf{e}\mathbf{v_s} & \text{if } \mathbf{v_s} \perp \mathbf{v_e} \end{cases}, \tag{67}$$

these properties are visualized in Figure 5.

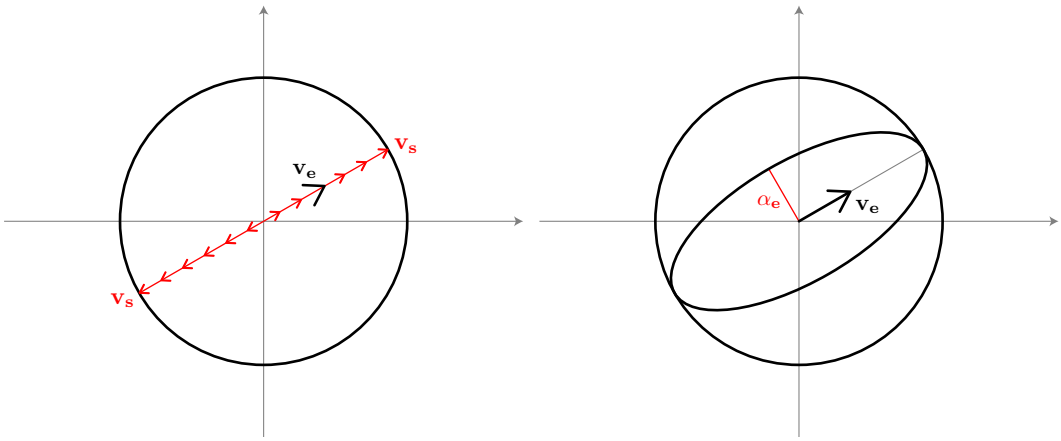


Figure 5: *Left*: all Bloch vectors $\mathbf{v_s}$ collinear with $\mathbf{v_e}$ are left fixed by $\mathcal{L}_\mathbf{e}$. *Right*: $\mathcal{L}_\mathbf{e}$ shrinks the Bloch vectors $\mathbf{v_s}$ orthogonal to $\mathbf{v_e}$ by the quantity $\alpha_\mathbf{e}$.

Since all states $\mathbf{s}$ with Bloch vector collinear with the effect vector are fixed by $\mathcal{L}_\mathbf{e}$, this holds true also for pure states. This fact implies that the two points defined by the intersection between the circle $S^1$ and the diameter of $\mathcal{D}$ collinear with $\mathbf{v_e}$ are fixed by $\mathcal{L}_\mathbf{e}$. The rebit channels classification guarantees that the only channels that preserve pure states are either the identity or the phase-flip channels of type $(1, 1-p)$ or $(1-p, 1)$, $p \in (0, 1]$, possibly degenerated into linear channels.

Coherently with the general analysis outlined before, $\mathcal{L}_\mathbf{e}$ is the identity when $\mathbf{e}$ is a neutral effect, i.e. when $\mathbf{v_e} = \mathbf{0}$, independently of $e_0 \in (0, 1)$, because in this case $\alpha_\mathbf{e} = 1$ and eq. (66) implies $\mathbf{v}_{\mathcal{L}_\mathbf{e}(\mathbf{s})} = \mathbf{v_s}$, so $\mathcal{L}_\mathbf{e}(\mathbf{s}) = \mathbf{s}$ for all state $\mathbf{s}$.

Instead, if $\mathbf{v_e} \neq \mathbf{0}$, then $\alpha_\mathbf{e} \in [0, 1)$ and so $\mathcal{L}_\mathbf{e}$ is a phase-flip channel with major and minor semi-axes, respectively, with lengths

$$\lambda_i = 1 \quad \text{and} \quad \lambda_k = \alpha_\mathbf{e} \in [0, 1), \qquad i, k \in \{1, 2\},\ i \neq k, \tag{68}$$

where the major axis always lies in the same direction as $\mathbf{v_e}$, which remains fixed.

Finally, if $\mathbf{e}$ is an extremal channel, then $\alpha_\mathbf{e} = 0$ and the phase-flip channel $\mathcal{L}_\mathbf{e}$ degenerates into a linear channel with $\lambda_i = 1$ and $\lambda_k = 0$, $i, k \in \{1, 2\}$, $i \neq k$.

The following theorem resumes the analysis just performed.

**Theorem 4.1** *Given $\mathbf{e} \in \mathcal{E}$, the 1-Lüders channel $\mathcal{L}_\mathbf{e}$ fixes any rebit state $\mathbf{s}$ whose Bloch vector is collinear with $\mathbf{v_e}$ and it is*

- *the identity, if $\mathbf{e}$ is a neutral effect*
- *a phase-flip channel degenerated into a linear one, if $\mathbf{e}$ is an extremal effect*
- *a phase-flip channel of type $(1, \alpha_\mathbf{e})$ or $(\alpha_\mathbf{e}, 1)$, otherwise.*

This theorem implies that the rebit channels that can be represented by 1-Lüders channels are only those parameterized by the points $(\lambda_1, \lambda_2) \in \mathcal{P}$ highlighted in red in Figure 6.

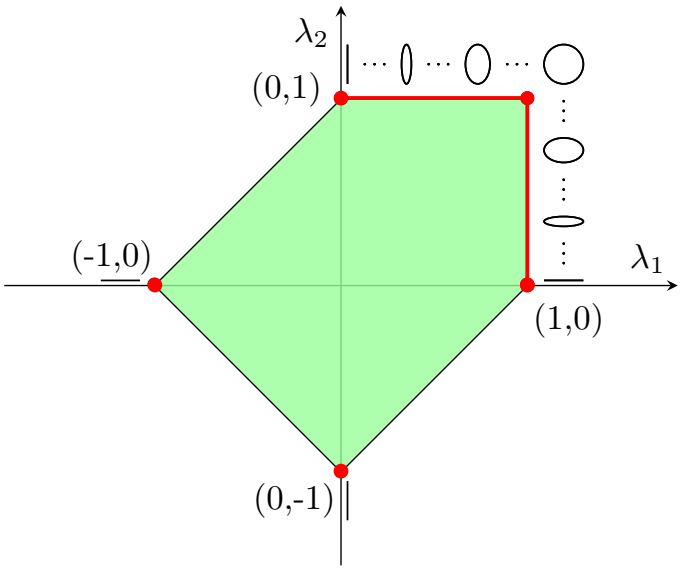


Figure 6: The parameters corresponding to rebit channels in the admissibility region that can be represented by 1-Lüders channels are highlighted in red. As depicted, they evolve from degenerated phase-flip channels to the identity. Up to a rotation, the parameters with coordinates $(-1, 0)$ and $(0, -1)$ give rise to the same degenerated phase-flip channels as those with coordinates $(1, 0)$ and $(0, 1)$, respectively.

Eq. (29) becomes particularly simple for 1-Lüders channels:

$$\mathbf{v}_{\mathcal{L}_\mathbf{e}(\mathbf{s})} = \alpha_\mathbf{e}\mathbf{v}_\mathbf{s} + \beta_{\mathbf{e},\mathbf{s}}(1-\alpha_\mathbf{e})\mathbf{v}_\mathbf{e}, \tag{69}$$

and it permits to highlight the geometric way in which $\mathcal{L}_\mathbf{e}$ transforms Bloch vectors, namely:

$$(\mathbf{v}_\mathbf{s} - \mathbf{v}_{\mathcal{L}_\mathbf{e}(\mathbf{s})}) \perp \mathbf{v}_\mathbf{e}, \tag{70}$$

which can be proven directly as follows

$$\begin{aligned} \mathbf{v}_\mathbf{e} \cdot (\mathbf{v}_\mathbf{s} - \mathbf{v}_{\mathcal{L}_\mathbf{e}(\mathbf{s})}) &= \mathbf{v}_\mathbf{e} \cdot \mathbf{v}_\mathbf{s} - \mathbf{v}_\mathbf{e} \cdot \mathbf{v}_{\mathcal{L}_\mathbf{e}(\mathbf{s})} = \mathbf{v}_\mathbf{e} \cdot \mathbf{v}_\mathbf{s} - \alpha_\mathbf{e}\mathbf{v}_\mathbf{e} \cdot \mathbf{v}_\mathbf{s} - \beta_{\mathbf{e},\mathbf{s}}(1-\alpha_\mathbf{e})\|\mathbf{v}_\mathbf{e}\|^2 \\ &= \mathbf{v}_\mathbf{e} \cdot \mathbf{v}_\mathbf{s} - \alpha_\mathbf{e}\mathbf{v}_\mathbf{e} \cdot \mathbf{v}_\mathbf{s} - (1-\alpha_\mathbf{e})\mathbf{v}_\mathbf{e} \cdot \mathbf{v}_\mathbf{s} = 0. \end{aligned} \tag{71}$$

Figure 7 visualizes the previous formula.

We conclude the analysis of 1-Lüders channels with the explicit computation of the von Neumann entropy of $\mathcal{L}_\mathbf{e}(\mathbf{s})$. The density matrix associated to $\mathcal{L}_\mathbf{e}(\mathbf{s})$ is

$$\rho_{\mathcal{L}_\mathbf{e}(\mathbf{s})} = \begin{pmatrix} 1 + \alpha_\mathbf{e}s_1 + \beta_{\mathbf{e},\mathbf{s}}(1-\alpha_\mathbf{e})\frac{e_1}{e_0} & \alpha_\mathbf{e}s_2 + \beta_{\mathbf{e},\mathbf{s}}(1-\alpha_\mathbf{e})\frac{e_2}{e_0} \\ \alpha_\mathbf{e}s_2 + \beta_{\mathbf{e},\mathbf{s}}(1-\alpha_\mathbf{e})\frac{e_2}{e_0} & 1 - \alpha_\mathbf{e}s_1 - \beta_{\mathbf{e},\mathbf{s}}(1-\alpha_\mathbf{e})\frac{e_1}{e_0} \end{pmatrix},$$

and its eigenvalues are

$$\mu_{1,2} = \frac{1 \pm \|\alpha_\mathbf{e}\mathbf{v}_\mathbf{s} + \beta_{\mathbf{e},\mathbf{s}}(1-\alpha_\mathbf{e})\mathbf{v}_\mathbf{e}\|}{2},$$

thus, by eq. (4), we obtain

$$\begin{aligned} S(\mathcal{L}_\mathbf{e}(\mathbf{s})) &= -\frac{1 - \|\alpha_\mathbf{e}\mathbf{v}_\mathbf{s} + \beta_{\mathbf{e},\mathbf{s}}(1-\alpha_\mathbf{e})\mathbf{v}_\mathbf{e}\|}{2} \log_2 \frac{1 - \|\alpha_\mathbf{e}\mathbf{v}_\mathbf{s} + \beta_{\mathbf{e},\mathbf{s}}(1-\alpha_\mathbf{e})\mathbf{v}_\mathbf{e}\|}{2} \\ &\quad - \frac{1 + \|\alpha_\mathbf{e}\mathbf{v}_\mathbf{s} + \beta_{\mathbf{e},\mathbf{s}}(1-\alpha_\mathbf{e})\mathbf{v}_\mathbf{e}\|}{2} \log_2 \frac{1 + \|\alpha_\mathbf{e}\mathbf{v}_\mathbf{s} + \beta_{\mathbf{e},\mathbf{s}}(1-\alpha_\mathbf{e})\mathbf{v}_\mathbf{e}\|}{2} \\ &= 1 - \frac{1}{2}\log_2\left(1 - \|\alpha_\mathbf{e}\mathbf{v}_\mathbf{s} + \beta_{\mathbf{e},\mathbf{s}}(1-\alpha_\mathbf{e})\mathbf{v}_\mathbf{e}\|^2\right) \\ &\quad - \frac{1}{2}\|\alpha_\mathbf{e}\mathbf{v}_\mathbf{s} + \beta_{\mathbf{e},\mathbf{s}}(1-\alpha_\mathbf{e})\mathbf{v}_\mathbf{e}\| \log_2 \frac{1 + \|\alpha_\mathbf{e}\mathbf{v}_\mathbf{s} + \beta_{\mathbf{e},\mathbf{s}}(1-\alpha_\mathbf{e})\mathbf{v}_\mathbf{e}\|}{1 - \|\alpha_\mathbf{e}\mathbf{v}_\mathbf{s} + \beta_{\mathbf{e},\mathbf{s}}(1-\alpha_\mathbf{e})\mathbf{v}_\mathbf{e}\|}. \end{aligned} \tag{72}$$

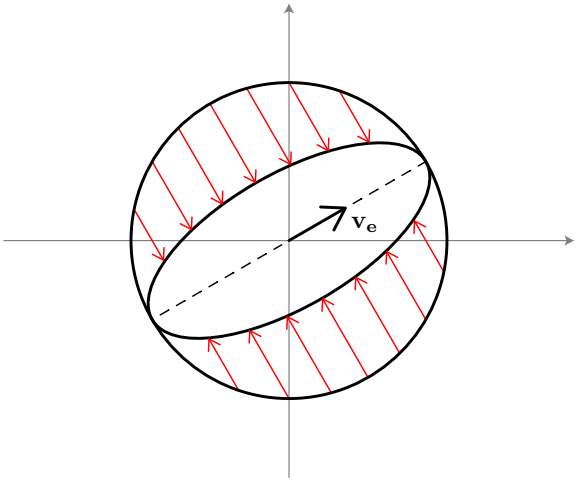


Figure 7: Geometric visualization of the pure states transformation by $\mathcal{L}_{\mathbf{e}}$ with respect to the effect vector $\mathbf{v_e}$.

## 4.2 2-Lüders channels

In the previous subsection we have showed that only a limited kind of rebit channels can be represented by 1-Lüders channels. In particular, they cannot account for depolarizing channels because the ellipsoidal region in which they transform the Bloch disk contains always the two antipodal points of $S^1$ determined by the direction of the effect vector.

In this subsection we will show explicitly that it is sufficient to consider $n \geq 2$ to represent *all kinds* of rebit channels (but not *all* rebit channels), including depolarizing ones, with $n$-Lüders channels.

To simplify the notation, instead of $\mathbf{e}_1, \mathbf{e}_2$, we will write $\mathbf{e} = (e_0, e_1, e_2)$ and $\mathbf{f} = (f_0, f_1, f_2)$, respectively.

When $\mathbf{v_e}$ and $\mathbf{v_f}$ are collinear, analogous computations as those performed in the case of 1-Lüders channels show that we can generate phase flip and linear rebit channels through 2-Lüders channels.

The following result shows what happens when $\mathbf{v_e}$ and $\mathbf{v_f}$ are orthogonal.

**Theorem 4.2** *Let $\mathcal{L}_{\mathbf{e},\mathbf{f}}$ be a 2-Lüders channel with $\mathbf{e}$ and $\mathbf{f}$ such that $\mathbf{v_e} \perp \mathbf{v_f}$. Then $\mathcal{L}_{\mathbf{e},\mathbf{f}}$ shrinks the Bloch disk into a 2-dimensional ellipsoid with semi-axes directed as $\mathbf{v_e}$ and $\mathbf{v_f}$ and with lengths*

$$\lambda_{\mathbf{f}} = \frac{1}{2}(1 + \alpha_{\mathbf{f}}) \in \left[\frac{1}{2}, 1\right] \qquad \textit{and} \qquad \lambda_{\mathbf{e}} = \frac{1}{2}(1 + \alpha_{\mathbf{e}}) \in \left[\frac{1}{2}, 1\right], \tag{73}$$

*respectively, where $\lambda_{\mathbf{f}} = 1$ (respectively, $\lambda_{\mathbf{e}} = 1$) if and only if $\mathbf{f}$ (respectively, $\mathbf{e}$) is a neutral effect. Moreover, if $e_0 = f_0$ and $\|\mathbf{v_e}\| = \|\mathbf{v_f}\|$, then the ellipsoids are disks with radius $\lambda_{\mathbf{f}} = \lambda_{\mathbf{e}}$.*

*Proof.* Since $\mathbf{v_e}$ and $\mathbf{v_f}$ are orthogonal, up to a rotation, we can always consider a coordinate system where $\mathbf{v_e}$ and $\mathbf{v_f}$ coincide with the horizontal and vertical axis, respectively. With this choice, $\vartheta_{\mathbf{e}} = 0$ and $\vartheta_{\mathbf{f}} = \pi/2$, so the coefficients $b_{\mathbf{e},\mathbf{f}}$ appearing in formula (48) are always null, while

$$a_{\mathbf{e},\mathbf{f}} = \frac{1}{2}(\alpha_{\mathbf{e}} + (1 - \alpha_{\mathbf{e}}) + \alpha_{\mathbf{f}}) = \frac{1}{2}(1 + \alpha_{\mathbf{f}}) \tag{74}$$

and

$$b_{\mathbf{e},\mathbf{f}} = \frac{1}{2}(\alpha_{\mathbf{e}} + \alpha_{\mathbf{f}} + (1 - \alpha_{\mathbf{f}})) = \frac{1}{2}(1 + \alpha_{\mathbf{e}}), \tag{75}$$

so

$$\mathbf{v}_{\mathcal{L}_{\mathbf{e},\mathbf{f}}(\mathbf{s})} = \frac{1}{2}\begin{pmatrix}(1 + \alpha_{\mathbf{f}})\, r_{\mathbf{s}} \cos\vartheta_{\mathbf{s}} \\ (1 + \alpha_{\mathbf{e}})\, r_{\mathbf{s}} \sin\vartheta_{\mathbf{s}}\end{pmatrix}. \tag{76}$$

The components of $\mathbf{v}_{\mathcal{L}_{\mathbf{e},\mathbf{f}}(\mathbf{s})}$ give the parametric representation of an ellipse with semi-axes of length $\lambda_{\mathbf{f}} = (1+\alpha_{\mathbf{f}})/2$ in the direction of $\mathbf{v}_{\mathbf{e}}$ and $\lambda_{\mathbf{e}} = (1+\alpha_{\mathbf{e}})/2$ in the direction of $\mathbf{v}_{\mathbf{f}}$. Since $\alpha_{\mathbf{e}}, \alpha_{\mathbf{f}} \in [0,1]$, with the value 1 reached only in the case of a neutral effect, we have the first statement of the theorem. In the particular case $e_0 = f_0$ and $\|\mathbf{v}_{\mathbf{e}}\| = \|\mathbf{v}_{\mathbf{f}}\|$, we have $\lambda_{\mathbf{e}} = \lambda_{\mathbf{f}}$ and the ellipse becomes a circle with radius $\lambda_{\mathbf{e}} = \lambda_{\mathbf{f}}$. □

Figure 8 shows explicitly that, even if *all types* of rebit channels can be represented by $n$-Lüders channels starting by $n = 2$, not *all* rebit channels can be represented by 2-Lüders channels,

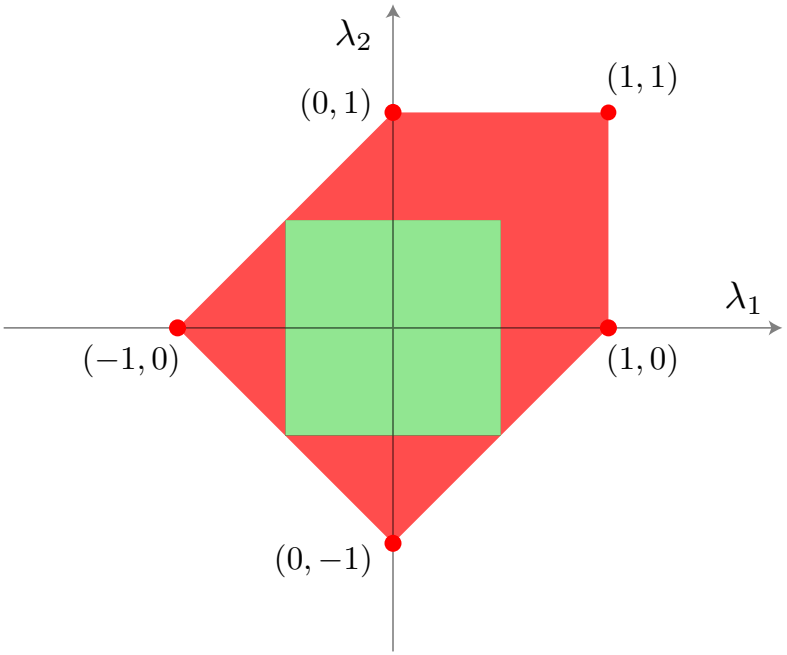


Figure 8: The red region represents the parameters of rebit channels that can be represented as 2-Lüders channels, to be compared with those appearing in Figure 6.

The maximal depolarization achievable in the case $n = 2$ is reached when $\alpha_{\mathbf{e}} = \alpha_{\mathbf{f}} = 0$, i.e. when both $\mathbf{e}$ and $\mathbf{f}$ are extremal effects. In such a case, the Bloch disk is shrunk into a disk of radius $1/2$.

Figure 9 shows a 2-Lüders channel acting as a generic phase flip channel and as the maximal depolarizing channel.

For 2-Lüders channels with orthogonal effect vectors, the relation in eq. (70) becomes more complicated:

$$(\mathbf{v}_{\mathbf{e}} + \mathbf{v}_{\mathbf{f}}) \cdot (\mathbf{v}_{\mathbf{s}} - \mathbf{v}_{\mathcal{L}_{\mathbf{e},\mathbf{f}}(\mathbf{s})}) + \mathbf{v}_{\mathbf{s}} \cdot (\alpha_{\mathbf{f}}\mathbf{v}_{\mathbf{e}} + \alpha_{\mathbf{e}}\mathbf{v}_{\mathbf{f}}) = 0, \tag{77}$$

which, when both $\mathbf{e}$ and $\mathbf{f}$ are extremal effects, simplifies to

$$(\mathbf{v}_{\mathbf{e}} + \mathbf{v}_{\mathbf{f}}) \perp (\mathbf{v}_{\mathbf{s}} - \mathbf{v}_{\mathcal{L}_{\mathbf{e},\mathbf{f}}(\mathbf{s})}), \quad \mathbf{e},\mathbf{f} \text{ extremal and } \mathbf{v}_{\mathbf{e}} \perp \mathbf{v}_{\mathbf{f}}, \tag{78}$$

and when $\mathbf{e}$ and $\mathbf{f}$ are neutral effects it becomes

$$(\mathbf{v}_{\mathbf{e}} + \mathbf{v}_{\mathbf{f}}) \perp (2\mathbf{v}_{\mathbf{s}} - \mathbf{v}_{\mathcal{L}_{\mathbf{e},\mathbf{f}}(\mathbf{s})}), \quad \mathbf{e},\mathbf{f} \text{ neutral and } \mathbf{v}_{\mathbf{e}} \perp \mathbf{v}_{\mathbf{f}}. \tag{79}$$

# 5 Application to the quantum model of color perception

In this section we discuss a first proposal for the application of $n$-Lüders channels and their properties to the quantum color perception theory which, as recalled in the introduction, originated the need for the classification of rebit channels and, consequently, the interest about $n$-Lüders channels. We start by briefly recalling the basic characteristics of this model.

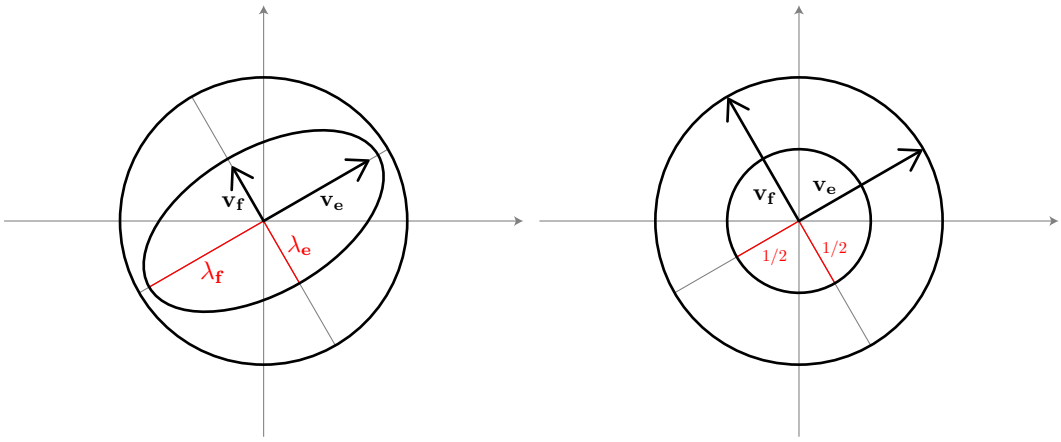


Figure 9: *Left*: $\mathcal{L}_{\mathbf{e},\mathbf{f}}$ acting as a generic phase-flip channel. *Right*: $\mathcal{L}_{\mathbf{e},\mathbf{f}}$ acting as the maximal depolarizing channel.

## 5.1 A basic recap of the quantum color perception quantum

As anticipated in the introduction, Schrödinger, see [24], condensed the fragmented knowledge about the space of perceptual colors $\mathcal{C}$ into a set of axioms which imply that the space of perceptual colors $\mathcal{C}$ is a 3-dimensional regular convex cone. In [22], Resnikoff completed Schrödinger's axiomatic system with a homogeneity axiom which implies that $\mathcal{C}$ can only take two forms: either $\mathbb{R}^+ \times \mathbb{R}^+ \times \mathbb{R}^+$ or $\mathbb{R}^+ \times \mathbf{H}$, where $\mathbf{H}$ is a 2-dimensional hyperbolic space with constant negative curvature -1, see e.g. [20] for a more modern introduction about Resnikoff's work.

It is very important to stress that $\mathcal{C}$ represents an *ideal space of perceptual colors in isolation*, meaning that $\mathcal{C}$ contains all the possible color sensations reported by an average observer who senses a single light source in isolation, without considering the real limitations of human vision with respect to light intensity.

The space $\mathbb{R}^+ \times \mathbb{R}^+ \times \mathbb{R}^+$ is the prototype of the classical CIE (Commission International de l'Éclairage) color spaces, which is known not to be able to take into account perceptual phenomena, whereas $\mathbb{R}^+ \times \mathbf{H}$ is a much more interesting space from an algebraic, geometric and perceptual point of view. $\mathbb{R}^+ \times \mathbf{H}$ is isomorphic to $\overline{\mathcal{H}^+}(2,\mathbb{R})$, the space of $2 \times 2$ positive-semidefinite real symmetric matrices, and to $\overline{\mathcal{L}^+}$, the closure of the future lightcone in the 3-dimensional Minkowski space. From now on, we will identify $\mathcal{C}$ with either one of these two spaces, which coincide precisely with *the domain of positivity of the only two non-associative 3-dimensional formally real Jordan algebras*: $\mathcal{H}(2,\mathbb{R})$, composed by real symmetric $2 \times 2$ matrices and endowed with the Jordan product $A \circ B = (AB + BA)/2$, where $A, B \in \mathcal{H}(2,\mathbb{R})$, and $\mathbb{R} \oplus \mathbb{R}^2$, the so-called *spin factor*, equipped with the product $(\alpha, \mathbf{v}) \circ (\beta, \mathbf{w}) = (\alpha\beta + \langle \mathbf{v}, \mathbf{w} \rangle, \alpha\mathbf{w} + \beta\mathbf{v})$, where $\alpha, \beta \in \mathbb{R}$ and $\mathbf{v}, \mathbf{w} \in \mathbb{R}^2$.

This assumption about $\mathcal{C}$ is called *trichromacy axiom* in [4], because it is the mathematical translation of the trichromatic nature of human color perception due to the existence of three retinal photoreceptors with different sensitivities. However, it is a well-known physiological fact that, while photoreceptors *allow* color vision, ganglion cells and other retinal neurons *generate* color vision via the opponent mechanism first argued by Hering [16]. Thus, the properties of a perceptual color space should be able to account for *both trichromacy and opponency*. As we are going to see, analyzing color perception from a quantum viewpoint permits to intrinsically account for both trichromacy and opponency.

Quantum states in this framework are called *chromatic states* and the associated density matrices are unit trace elements of $\overline{\mathcal{H}^+}(2,\mathbb{R})$, which coincide exactly with the matrices appearing in eq. (1), i.e. those of a rebit system, hence they can be parameterized by the points of the Bloch disk $\mathcal{D} \subset \mathbb{R}^2$. We stress that the only assumption behind *the spontaneous appearance of a rebit system when studying color perception* is the quantum interpretation of the trichromacy axiom.

We also notice that the dimensional reduction from 3 (trichromacy) to 2 (parameters labeling

rebit states) is far from being an accidental, or even unwanted, feature of this model: D. Hubel masterfully resumed in [17] the spirit of Hering's opponent color theory by stating that the only intrinsic information that can be extracted by the observation of color in isolated conditions is represented by the two degrees of chromatic opposition, while the perceived intensity, or brightness, needs comparisons with other color stimuli.

The two degrees of opposition are exhibited by the density matrices when their Bloch representation, eq. (2), is written in polar coordinates, see [4], i.e. $(s_1, s_2) = (r\cos\vartheta, r\sin\vartheta)$, $r \in [0,1]$, $\vartheta \in [0, 2\pi)$:

$$\rho_{\mathbf{s}}(r,\theta) = \rho_0 + \frac{r\cos\theta}{2}\left[\rho_{\mathbf{s}}(1,0) - \rho_{\mathbf{s}}(1,\pi)\right] + \frac{r\sin\theta}{2}\left[\rho_{\mathbf{s}}\left(1,\pi/2\right) - \rho_{\mathbf{s}}\left(1,3\pi/2\right)\right]. \tag{80}$$

It turns out that, for all $\vartheta \in [0, 2\pi)$, $\rho_{\mathbf{s}}(1,\vartheta)$ is a rank-1 projector, i.e. a *pure state*, and $\rho_{\mathbf{s}}(1,\vartheta_1)$, $\rho_{\mathbf{s}}(1,\vartheta_2)$ project on orthogonal directions precisely when $\vartheta_1$ and $\vartheta_2$ are antipodal, a feature common to rebits and qubits, but which fails to be true in higher dimensions. Since orthogonality in quantum theories represents incompatible states, eq. (80) codifies a generic chromatic state with the presence of two opponencies between incompatible states, red-green and yellow-blue in Hering's theory, plus an offset state represented by $\rho_0$, called *achromatic state*, characterized by the fact of maximizing the von Neumann entropy and not carrying any chromatic information. This is precisely the translation of Hering's color theory in terms of rebit states and this is the reason why this system is called *Hering's rebit*. The corresponding Bloch disk is depicted in Figure 10.

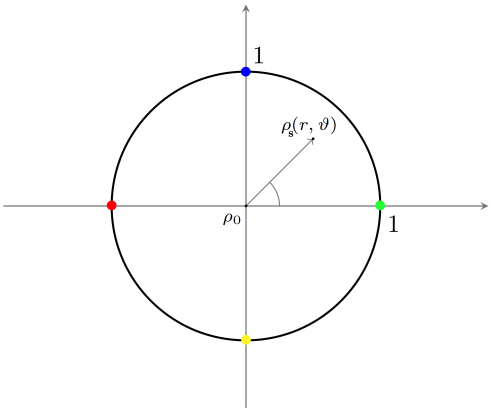


Figure 10: The space of chromatic states of Hering's rebit with the antipodal chromatic opposition exhibited.

Finally, we mention that the saturation $\Sigma$ of the chromatic state $\mathbf{s}$ is defined either as 1 minus the von Neumann entropy of $\rho_{\mathbf{s}}$, or, equivalently, as the relative entropy $R$ of $\rho_{\mathbf{s}}$ w.r.t. the achromatic state $\rho_0$:

$$\Sigma(\mathbf{s}) = 1 - S(\mathbf{s}) = R(\rho_{\mathbf{s}}||\rho_0) = \frac{1}{2}\log_2(1 - r_{\mathbf{s}}^2) + \frac{r_{\mathbf{s}}}{2}\log_2\frac{1+r_{\mathbf{s}}}{1-r_{\mathbf{s}}}, \tag{81}$$

see [8] for more details.

## 5.2 $n$-Lüders channels and color perception

Let us now discuss how the actual interaction between an observer and a color stimulus can be analyzed using channels and, more generally, the mathematical language of quantum information of open systems.

In the quantum-like color framework, the act of perceiving a color by the visual system of a human observer is modeled via a (perceptual) measurement, see [10, 8]. In the theory of quantum

information, a channel is interpreted as the 'medium' which transmits an initial state to a modified one. When the modification follows from the act of observation, it seems reasonable to assume that the associated quantum channel is a suitable $n$-Lüders channel $\mathcal{L}_{\mathbf{e}_1,\dots,\mathbf{e}_n}$ of Hering's rebit, since effects codify the probabilistic nature of quantum measurement.

Each observer $\mathbf{o}$ gathers chromatic information performing perceptual measurements through the effects $\mathbf{e}_1,\dots,\mathbf{e}_n$ that are accessible thanks to the personal characteristics of the visual system of $\mathbf{o}$. This allows $\mathbf{o}$ to reconstructs her/his individual chromatic state space $\mathcal{C}_\mathbf{o}$ as the range of the corresponding $n$-Lüders channel, i.e. $\mathcal{C}_\mathbf{o} = \mathcal{L}_{\mathbf{e}_1,\dots,\mathbf{e}_n}(\mathcal{S}(\mathbb{R}^2))$.

A neutral effect $\mathbf{e}$ in this context is called an *achromatic effect* and it is indicated with $\mathbf{e_a}$ because, if interpreted as a chromatic vector, it corresponds to the center of the Bloch disk, where the achromatic state $\rho_0$ is situated. The analysis performed in section 4 showed that, if $\mathbf{e}_1 = \dots = \mathbf{e}_n = \mathbf{e_a}$, then $\mathcal{L}_{\mathbf{e_a},\dots,\mathbf{e_a}}(\mathcal{S}(\mathbb{R}^2)) = \mathcal{S}(\mathbb{R}^2)$.

As we will see in the following subsections, $C_\mathbf{o}$ can also account for color perception deficiencies, for this reason it is worth recalling some standard definitions form ophthalmology and color theory:

- the LMS cones are the retinal photoreceptors with sensitivity pick in the long, middle and short wavelengths of the visual spectrum. Apart from the separation of their picks, the sensitivity curves of the L and M cones are almost identical and they vastly overlap;
- a *normal trichromatic observer* is a person with the three LMS cones functioning and with maxima of their absorption curves at 560, 530 and 420 nm, respectively;
- an *anomalous trichromatic observer* is a person with the three LMS cones functioning, but the absorption curves maxima of the L and M cones are less separated, typically between 2 and 12 nm, far less than the 30 nm separation of normal trichromats. This is the most common color deficiency found in humans. We further distinguish between the two following sub-categories: *protanomalous* have normal S and M cones, but anomalous L cones whose spectral sensitivity curve is shifted closer to that of M cones; *deuteranomalous* have normal S and L cones, but anomalous M cones whose spectral sensitivity curve is shifted closer to that of L cones[3];
- a dichromatic observer is a person who lacks one type of cones. We distinguish among: *protanopes*, who lack the L cones; *deuteranopes*, who lack the M cones; *tritanopes*, who lack the S cones[4];
- a *monochromatic observer* is a person affected by a very rare color deficiency in which only the S cones are functioning or no cones at all, in which case they only possess skotopic vision via the rod system. These people totally lack chromatic sensation.

## 5.3 Individual chromatic state space from 1-Lüders channels, the dichromatic case

In the case of 1-Lüders channels we only have at disposal one effect $\mathbf{e} = (e_0, \mathbf{v_e})$, with magnitude $e_0 \in (0,1)$, and vector $\mathbf{v_e} \in \mathcal{D}$ and the induced effect $\mathbb{1}-\mathbf{e}$, with magnitude $1-e_0 \in (0,1)$ and vector $\mathbf{v}_{\mathbb{1}-\mathbf{e}} = -\dfrac{e_0}{1-e_0}\mathbf{v_e} \in \mathcal{D}$, collinear with $\mathbf{v_e}$. Hence, observers characterized by 1-Lüders channels can only perform perceptual measurements in one particular chromatic axis of opponency[5]: it is the case of dichromats.

Since it is known that chromatic perception of dichromats is limited, we exclude a priori the possibility that a dichromat observer has access to the achromatic effect $\mathbf{e_a}$, which would lead to a perfect preservation of the Bloch disk. Instead, we examine these possibilities:

[3] data on people with a shifted S cone spectral sensitivity have not been confirmed solidly.

[4] the prefixes used in these definitions and the following one are derived from *protos*, *deuteros* and *tritos*, which mean first, second and third, respectively, in ancient Greek.

[5] recall that, in Hering's theory, only the measurement of chromatic opponency has an intrinsic meaning for isolated color stimuli.

- if the observer $\mathbf{o}$ can perform perceptual measures with the extremal effect $\mathbf{e}$, i.e. $\|\mathbf{v_e}\| = 1$ and $e_0 = 1/2$, then $\mathcal{L}_\mathbf{e}$ is a degenerate phase-flip channel of type $(0,1)$ or $(1,0)$, so $\mathcal{L}_\mathbf{e}$ makes $\mathcal{C}_\mathbf{o}$ collapse to the diameter of the Bloch disk defined by $\mathbf{v_e}$. This describes the most severe case of dichromatism. Referring to the color configuration of Figure 10, we have that:
  - a *perfect protanope* or a *perfect deuteranope* is described by a degenerate phase-flip channel of type $(0,1)$;
  - a *perfect tritanope* is described by a degenerate phase-flip channel of type $(1,0)$;
- if the observer $\mathbf{o}$ can perform perceptual measures with an effect $\mathbf{e}$ which is intermediate between the neutral and the extremal, then $\mathcal{C}_\mathbf{o}$ becomes a 2D ellipsoid with major axis directed as $\mathbf{v_e}$ and length 1 and with minor axis with length $\alpha_\mathbf{e}$, see Figure 5 on the right. This corresponds to a less severe dichromatism, characterized by a reduced ability of distinguishing among differently saturated colors not belonging to the opponent axis defined by $\mathbf{v_e}$ modulated by the value of $\alpha_\mathbf{e}$: the smaller $\alpha_\mathbf{e}$, the more pronounced the lack of saturation distinguishability. Since 1-Lüders channels cannot reproduce depolarizing channels, the loss in ability to distinguish color saturation is always greater for colors whose chromatic states do not belong to the diameter defined by $\mathbf{v_e}$ and it is maximal in the orthogonal direction.

Thanks to eq. (72), the saturation of a states $\mathbf{s}$ modified by a 1-Lüders channel is

This analysis is qualitatively coherent with the data reported e.g. by Emery et al. in [13], which show that dichromats are able to perceive far more chromatic sensations than generally thought, but they have more trouble distinguishing colors with similar saturation than normal trichromats.

### 5.4 Individual chromatic state space from 2-Lüders channels, the case of anomalous trichromats

Observers characterized by 2-Lüders channels can perform perceptual measurements along two chromatic axes of opponency: it is the case of trichromats or anomalous trichromats. Thanks to the analysis detailed in section 4.2, we know that a perfect normal trichromat acts on the Bloch disk with the channel $\mathcal{L}_{\mathbf{e_a},\mathbf{e_a}}$, while in any other circumstance the chromatic state space will be shrunk into an 2D ellipsoid or a disk with radius belonging to the interval $[1/2, 1)$.

A tentative explanation for the appearance of a lower bound may lie in the fact that a $n$-Lüders channel is a superposition of selective measurements related to the effects $\mathbf{e}_1, \ldots, \mathbf{e}_n$ from which an observer gains information about the chromatic states. The mathematical analysis performed in this document shows that the information achieved always allows an observer to access to at least a finite amount of states. This may explain why dichromats are not color-blind as incorrectly thought. Instead, achromatic (totally color-blind) observers are not encompassed by $n$-Lüders channels.

Importantly, due to the non-linearity of the von Neumann (or of the relative) entropy, the difference in saturation perception of observers associated to channels that shrink the Bloch disk to even just a half is highly reduced, see Figure 11. Again, this is qualitatively coherent with the fact that observers with color perception deficiencies declare a degradation in their ability to perceive saturation differences that, for severe forms of dichromatic vision, can indeed be strong.

## 6 Conclusions

We have shown that, starting from $n$ quantum effects and the Lüders operations that they induce, it is possible to construct a novel class of rebit quantum channels. We have called them $n$-Lüders channels and performed a complete analysis of their properties by using some results proven in [10] and also to the classification of rebit channels recently completed in [1].

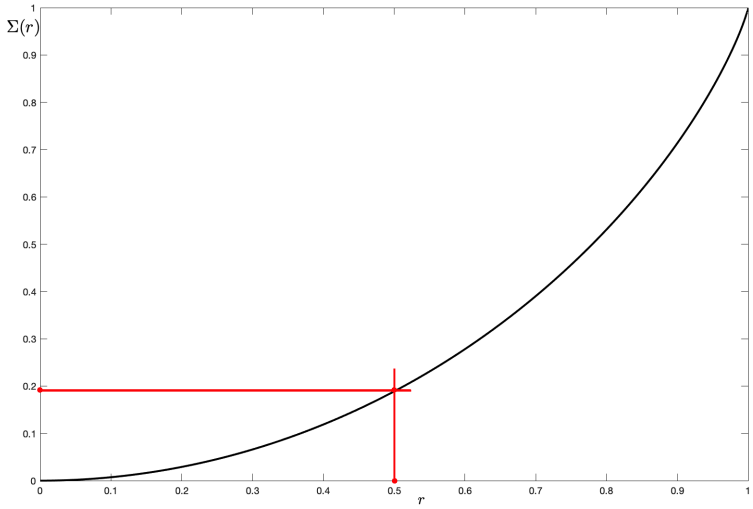


Figure 11: The saturation curve is depicted in black. When the radius $r$ of the Bloch disk is reduced to $1/2$, the corresponding value of the saturation $\Sigma(r)$ is diminished to less than 0.2.

While 1-Lüders channels can only represent the identity or a phase-flip channel (possibly degenerated into a linear one), $n$-Lüders channels with $n \geq 2$ can represent all types of rebit channels, but not all of them, because of the presence of a lower bound in their shrinking ability.

Finally, to show a concrete application of these novel concepts, we have discussed a possible use of $n$-Lüders channel within the theoretical framework that generated the exigence of the rebit channels classification, i.e. the quantum model of color perception described for instance in [8]. In particular, we have shown that if we define the individual chromatic state space of a human observer as the image of the Bloch disk by a $n$-Lüders channel, then we can describe also observers affected by human deficiencies in a way that appears in qualitative agreement with recent empirical studies, see e.g. [13].

Future perspective of the present work may include both the extension of the analysis of $n$-Lüders channels to qubit systems and the development of experimental protocols to tests our predictions about color deficiencies.

# References

[1] M. Aldé, M. Berthier, and E. Provenzi. The classification of rebit quantum channels. *Journal of Physics A: Mathematical and Theoretical*, 56(495301):1–17, 2023.

[2] Antoniya Aleksandrova, Victoria Borish, and William K Wootters. Real-vector-space quantum theory with a universal quantum bit. *Physical Review A*, 87(5):052106, 2013.

[3] John C Baez. Division algebras and quantum theory. *Foundations of Physics*, 42(7):819–855, 2012.

[4] M. Berthier. Geometry of color perception. Part 2: perceived colors from real quantum states and Hering's rebit. *The Journal of Mathematical Neuroscience*, 10(1):1–25, 2020.

[5] M. Berthier, V. Garcin, N. Prencipe, and E. Provenzi. The relativity of color perception. *Journal of Mathematical Psychology*, 103:102562, 2021.

[6] M. Berthier and E. Provenzi. When geometry meets psycho-physics and quantum mechanics: Modern perspectives on the space of perceived colors. In *International Conference on Geometric Science of Information 2019*, volume 11712 of *Lecture Notes in Computer Science*, pages 621–630. Springer Berlin-Heidelberg, 2019.

[7] M. Berthier and E. Provenzi. From Riemannian trichromacy to quantum color opponency via hyperbolicity. *Journal of Mathematical Imaging and Vision*, 63(6):681–688, 2021.

[8] Michel Berthier, Nicoletta Prencipe, and Edoardo Provenzi. A quantum information-based refoundation of color perception concepts. *SIAM Journal on Imaging Sciences*, 15(4):1944–1976, 2022.

[9] Michel Berthier and Edoardo Provenzi. The quantum nature of color perception: Uncertainty relations for chromatic opposition. *Journal of Imaging*, 7(40), 2021.

[10] Michel Berthier and Edoardo Provenzi. Quantum measurement and colour perception: theory and applications. *Proceedings of the Royal Society A*, 478(2258):20210508, 2022.

[11] Paul Busch, Marian Grabowski, and Pekka J Lahti. *Operational quantum physics*, volume 31. Springer Science & Business Media, 1997.

[12] Paul Busch, Pekka Lahti, Juha-Pekka Pellonpää, and Kari Ylinen. *Quantum measurement*, volume 23. Springer, 2016.

[13] Kara J Emery, Mohana Kuppuswamy Parthasarathy, Daniel S Joyce, and Michael A Webster. Color perception and compensation in color deficiencies assessed with hue scaling. *Vision Research*, 183:1–15, 2021.

[14] Christopher A Fuchs, Maxim Olchanyi, and Matthew B Weiss. Quantum mechanics? it's all fun and games until someone loses an $i$. *arXiv preprint arXiv:2206.15343*, 2022.

[15] Teiko Heinosaari and Mário Ziman. *The mathematical language of quantum theory: from uncertainty to entanglement*. Cambridge University Press, 2011.

[16] Ewald Hering. *Zur Lehre vom Lichtsinne: sechs Mittheilungen an die Kaiserl. Akademie der Wissenschaften in Wien*. C. Gerold's Sohn, 1878.

[17] D.H. Hubel. *Eye, Brain, and Vision*. Scientific American Library, 1995.

[18] Matthew McKague, Michele Mosca, and Nicolas Gisin. Simulating quantum systems using real Hilbert spaces. *Physical review letters*, 102(2):020505, 2009.

[19] Valter Moretti and Marco Oppio. Quantum theory in real hilbert space: How the complex hilbert space structure emerges from poincaré symmetry. *Reviews in Mathematical Physics*, 29(06):1750021, 2017.

[20] Edoardo Provenzi. Geometry of color perception. Part 1: Structures and metrics of a homogeneous color space. *The Journal of Mathematical Neuroscience*, 10(1):1–19, 2020.

[21] Marc-Olivier Renou, David Trillo, Mirjam Weilenmann, Thinh P Le, Armin Tavakoli, Nicolas Gisin, Antonio Acín, and Miguel Navascués. Quantum theory based on real numbers can be experimentally falsified. *Nature*, 600(7890):625–629, 2021.

[22] H.L. Resnikoff. Differential geometry and color perception. *Journal of Mathematical Biology*, 1:97–131, 1974.

[23] Mary Beth Ruskai, Stanislaw Szarek, and Elisabeth Werner. An analysis of completely-positive trace-preserving maps on M2. *Linear algebra and its applications*, 347(1-3):159–187, 2002.

[24] E. Schrödinger. Grundlinien einer Theorie der Farbenmetrik im Tagessehen (Outline of a theory of colour measurement for daylight vision). Available in English in Sources of Colour Science, Ed. David L. Macadam, The MIT Press (1970), 134-82. *Annalen der Physik*, 63(4):397–456; 481–520, 1920.

[25] Abraham Albert Ungar. *Analytic hyperbolic geometry and Albert Einstein's special theory of relativity*. World scientific, 2008.

[26] William K Wootters. Local accessibility of quantum states. *Complexity, entropy and the physics of information*, 8:39–46, 1990.

[27] William K Wootters. The rebit three-tangle and its relation to two-qubit entanglement. *Journal of Physics A: Mathematical and Theoretical*, 47(42):424037, 2014.